Published in final edited form as:
Ann Biomed Eng. 2013 July ; 41(7): 1347–1365. doi:10.1007/s10439-013-0800-z.

Physical Factors Effecting Cerebral Aneurysm Pathophysiology

Chander Sadasivan, **David J. Fiorella**, **Henry H. Woo**, and **Baruch B. Lieber***

Abstract

Many factors that are either blood-, wall-, or hemodynamics-borne have been associated with the initiation, growth, and rupture of intracranial aneurysms. The distribution of cerebral aneurysms around the bifurcations of the circle of Willis has provided the impetus for numerous studies trying to link hemodynamic factors (flow impingement, pressure, and/or wall shear stress) to aneurysm pathophysiology. The focus of this review is to provide a broad overview of such hemodynamic associations as well as the subsumed aspects of vascular anatomy and wall structure. Hemodynamic factors seem to be correlated to the distribution of aneurysms on the intracranial arterial tree and complex, slow flow patterns seem to be associated with aneurysm growth and rupture. However, both the prevalence of aneurysms in the general population and the incidence of ruptures in the aneurysm population are extremely low. This suggests that hemodynamic factors and purely mechanical explanations by themselves may serve as necessary, but never as necessary and sufficient conditions of this disease's causation. The ultimate cause is not yet known, but it is likely an additive or multiplicative effect of a handful of biochemical and biomechanical factors.

Keywords

cerebrovascular; hemodynamics; etiology; growth; rupture; geometry; flow patterns; wall shear stress

Introduction

Cerebral aneurysms are focal weakened pouches of arterial walls around bifurcations of the circle of Willis (Figure 1). Approximately 5% of the population (~15 million people in the United States) is estimated to have at least one cerebral aneurysm. About 0.2% of these aneurysms rupture every year (30,000 ruptures/year in the United States) leading to a subarachnoid hemorrhage.[33] This accounts for only about five percent of all strokes, but the consequences of aneurysmal hemorrhage are dire, carrying a mortality rate of about 50% and a morbidity rate among survivors of about 50%.[14] The pathophysiology (term used to include aneurysm formation, growth, and rupture unless otherwise specified) of aneurysms leading to aneurysm growth and eventual rupture are not entirely clear, but research, especially because of the large number of groups studying aneurysms over the past decade or two, continues to converge on identification of the mechanisms responsible.

Reasonably, such dilations occur because of deleterious factors or deficiencies in the blood or because of structural deficiencies in the arterial walls, or both, with the focal nature of the disease being modulated by normal or abnormal (yet undefined) hemodynamics at the predisposed locations (Figure 2). The extent to which the pathophysiology is intrinsically predisposed or environmentally induced is also not clear. Epidemiologically, factors

*Corresponding Author B. Barry Lieber, Professor, Department of Neurological Surgery, 100 Nicolls Road, HSC T12, Room 080, Stony Brook University Medical Center, Stony Brook, New York 11794-8122, Phone: 631-444-1278, baruch.lieber@sbumed.org.

associated with aneurysms over the years include smoking, excessive alcohol consumption, female gender post-menopause (potentially protective role of estrogen), polycystic kidney disease, Ehlers-Danlos syndrome, α1-antitrypsin deficiency, increased levels of plasma elastase, altered expression or activity of matrix metalloproteinases and tissue inhibitors of metalloproteinases, alterations in molecules involved in tissue repair/vascular remodeling/ extracellular matrix maintenance, growth factors, cellular adhesion molecules, familial history, genetic aberrations (genes or genetic regions encoding for collagens, elastin, endothelial nitric oxide synthase, α1-antitrypsin, matrix metalloproteinases (−1,−3,−9, and −12), tissue inhibitors of metalloproteinases, fibronectin, secreted protein acidic and rich in cysteine, polycystin, endoglin, transforming growth factor-β receptors, versican, perlecan, serpin, fibrillin), aneurysms with an irregular or multilobulated shape, aneurysms with higher aspect ratios (ratio of aneurysm height to neck), anomalies in the vascular tree around the circle of Willis, surgery or disease induced changes in flow in the affected parent artery, and larger aneurysm sizes[28,36,80,82,88,94,96,98,109,126,137,146,150,151,156,164,204]

The list is not exhaustive but is illustrative of the fact that a plethora of factors have been associated with aneurysms and that all of them are blood-, wall-, or hemodynamics-borne. More important, the evidence shows that taken individually, all these factors are at best proximate causes of aneurysm pathophysiology. In so far as hemodynamic factors (flow impingement, pressure, wall shear stress (WSS)) are concerned, the phenomenological/ epidemiological observation that the aneurysm occurrence rate is so low in the population demonstrates that these, by themselves, are insufficient conditions as causative factors of aneurysm initiation and formation. The ultimate cause is not yet known, but it is likely an additive or multiplicative effect of a handful of factors. Previous listed references may be consulted for cellular, molecular, and genetic factors associated with aneurysms. There are also several review articles written on the subject.[14,49,96,98,126,151,156,164,189,213] The focus of this review is to address hemodynamic factors associated with aneurysm pathophysiology; also addressed are anatomical and structural factors as these inherently affect prevailing hemodynamics. We attempt to provide an overview of the breadth of the subject so different aspects are dealt with in varying degrees of depth and we briefly summarize salient (due to importance or popular use) variables or articles and note our conclusions from the evidence presented. Thus, broadly, the article represents our perspective on the status of physical variables that govern aneurysm pathophysiology. The reader may look to the references listed to gain additional information on different aspects or to educate themselves on different perspectives.

A search of the phrase ‘(cerebral OR intracranial) AND aneurysm AND (flow OR hemodynamics)’ in Pubmed, Medline, and Compendex gave 2891, 2350, and 331 results, respectively; search of ‘(cerebral OR intracranial) AND aneurysm AND biomechanic*’ gave 85, 75, and 108, results respectively. Results were limited to journal articles, duplicates were removed, and article titles were manually reviewed to condense the number of articles to 386. The reference list used here is a representative subset of the content of these ~400 articles.

Geometry

Flow patterns at arterial locations predisposed to aneurysm formation or within aneurysms (predisposed to rupture) are intrinsically governed by vascular anatomy. Several studies have evaluated such anatomical and morphological factors with the goal of elucidating differences in vascular anatomy between patient and control populations to determine geometrical factors causing aneurysm initiation and between ruptured and unruptured aneurysms to determine geometrical factors causing aneurysm rupture. Table 1 summarizes the arterial locations within and around the circle of Willis at which aneurysms are found. It

should be noted that both ruptured and unruptured aneurysms are combined in the table and that the studies listed in the table may not precisely differentiate their results into the locations listed. For example, internal carotid aneurysms may include posterior communicating artery aneurysms while basilar artery aneurysms may include aneurysms of the vertebrobasilar system or list only basilar terminus aneurysms. The important point to note from the table, however, is that at least 70–75% of all intracranial aneurysms occur at one of three locations - the middle cerebral artery (at the bifurcation), the posterior communicating artery (at the internal carotid artery junction), and the anterior communicating artery (at the anterior cerebral artery junction). Internal carotid and basilar artery terminus aneurysms, which can be considered to be at 'T' junctions seem to constitute at most about 7% (at each terminus) of all aneurysms.[4,14,34,46,50,76,91,114,145]

A large number of geometrical studies are driven by the goal of determining thresholds that will delineate unruptured from ruptured aneurysms. Various variables have been suggested, of which the maximal aneurysm size is the most widely used. There were early suggestions that a critical size threshold varying between 5–10 mm existed above which aneurysms are at increased rupture risk, or at least that unruptured aneurysms smaller than 10 mm have very low probabilities of rupture.[31,207] But given the data collected thus far, this position does not seem defensible in so far as predicting rupture risk of any given unruptured aneurysm smaller than 10 mm. In general, the data clearly show that the average size of ruptured aneurysm samples is greater than the average size of unruptured aneurysm samples (Table 2). The effect size (ruptured size – unruptured size), however, seems to be about 1.5 mm at best. Also, 70–85% of all ruptured aneurysm samples are smaller than 10 mm.[9,46,76,78,125,204] Hypotheses suggesting that a certain class of aneurysms reach stability below the 10 mm size and thus rarely progress to rupture do not seem to be supported by the evidence.[46]

Other geometrical variables have been constructed to include the aneurysm-parent vessel complex in an attempt to derive better descriptors of rupture. The aspect ratio (aneurysm height/aneurysm neck) of ruptured aneurysm samples has been found to be ~2.4, while that of unruptured aneurysms ~1.6.[102,125,141,193] The size ratio (maximum aneurysm size/parent vessel diameter) of ruptured aneurysms is 4.1, while that of unruptured aneurysms, 2.6.[142] The volume orifice area ratio (aneurysm volume/aneurysm neck area) of ruptured aneurysms is 14 and that of unruptured aneurysms 7.[212] Ruptured aneurysms are often (40–60% of cases) multi-lobulated (presence of blebs) or have irregular surfaces.[31,59] Descriptors quantifying the shape of aneurysmal surfaces (surface undulations, ellipticity, non-sphericity, curvature) have also been found to have the potential to delineate ruptured from unruptured aneurysms.[34,141] Many other geometric variables have been constructed; the more popular ones have been reviewed previously.[4,102] The sensitivity of the predictive tests based on these factors is around 70–75%.[125,141,142,212] Much larger data sets will be required to improve the predictive value of these tests if they are to be used to make clinical prognoses of individual aneurysms. Also, geometrical thresholds predicting rupture would be more accurate if they were obtained from prospective studies of unruptured aneurysms that are left untreated and then progress to rupture instead of the retrospective data being used for these tests,[114,206] but such prospective studies are difficult to conduct.

Anomalies in the geometry of the circle of Willis (such as hypoplasia, absence, asymmetry of paired vessels, fenestrations, triplication) have been suggested to occur more frequently in patients with aneurysms as compared to controls.[12,91,208] Statements that no such differences exist have been made.[163] Contradictory reports have also been published associating circle of Willis anomalies with ruptured aneurysms.[34,105] Such anomalous circles of Willis seem to exist in about 50% of the general population.[84] The overall evidence seems to be insufficient to conclude such association at this time. However, there

does seem to be an association between asymmetry of the anterior cerebral arteries and the presence of anterior communicating artery aneurysms, with 25%–50% of circles with aneurysms having the asymmetry as compared to 5%–25% of non-aneurysmal circles.[91,115,163] There is marginal evidence indicating higher frequencies of asymmetry of the posterior communicating arteries in the patient population.[91] Aneurysms seem to be more (as compared to controls) prevalent at bifurcations with greater bifurcation angles (angle between the daughter branches).[12,73,89] The longitudinal axis (aneurysm height) of aneurysms is more aligned with the direction of parent vessel flow in ruptured aneurysms as compared to unruptured aneurysms.[4,34,153,177] There is some evidence that the longitudinal axis of aneurysms clusters around specific angles with respect to the parent artery[166] and that more distal aneurysms have smaller sizes,[17] but the effect of the perianeurysmal environment[154] must be considered along with such results. Advancements in software and hardware have enabled the quantification of much more sophisticated geometrical variables (or sophisticated combinations of geometrical variables) of the 3D aneurysm-parent vessel complex with relative ease[104,111,138,139] and although it is difficult to imagine that a critical threshold predicting aneurysm rupture (or initiation) could be derived from purely geometrical factors, future evaluation may yield a geometrical predictive test with acceptable sensitivity and specificity to be clinically useful.

Flow

Flow patterns and pressure

Flow in cerebral aneurysms has generally been evaluated qualitatively by clinical and in vivo angiography and dye visualization in glass and elastomeric models and quantitatively by particle image and laser Doppler velocimetry in glass and elastomeric models and by numerical computational fluid dynamic (CFD) simulations. Figure 3 is a sampling of images from such varied studies showing the fundamental patterns of flow within aneurysms; the reader may look into these and other references to gain additional visual perspective on intraneurysmal flow. As represented in the figure, the gross qualitative features of flow in all aneurysms can be discerned from knowing the geometry of the aneurysm-parent vessel complex and estimates of volumetric flow in the arteries leading to and from the aneurysm. The traditional flow pattern is that of sidewall aneurysms, where the flow near the vessel wall closer to the aneurysm impinges on the distal neck of the aneurysm, enters the aneurysm, moves along the aneurysm wall in a circular/vortical manner and exits the aneurysm back into the parent vessel at the proximal neck of the aneurysm.[51,67,71,110,135,168,169,180] Central regions of this vortex have very low flow activity.[53,128,136] This pattern, although simplistic, serves as a fundamental description of flow in all aneurysms. Complexity to the pattern is usually added by the prevailing geometry. Flow patterns in aneurysms at bifurcations, for example, are governed by the bifurcation angle, by the asymmetricity of the daughter branch diameters and by the flow distributions into these branches.[168] Flow from the parent artery tends to follow the trajectory along the longitudinal axis of the parent, tends to enter the aneurysm at the neck closer to the larger daughter branch, forms a vortex in the aneurysm, and exits at the opposite neck into the daughter branch closest to the exit.[136,175,192] The vortical structure may not be present if the aspect ratio of the aneurysm is very low (with flow maintaining its direction while deviating into the aneurysm) or a secondary vortex may form if the aspect ratio is high or if the aneurysm has a bleb.[110,135,192] Aneurysms with higher aspect ratios tend to have a lower ‘penetrance’ of flow or primary vortical structure into the aneurysm and tend to have flow stagnation zones near their domes.[147,192] Depending on the width and depth of this flow penetrance, a secondary vortex rotating in the opposite direction of the primary vortex may form in the aneurysm.[54,171] A greater part of the flow into anterior communicating artery aneurysms comes from the larger anterior cerebral artery but comprises of a mixing of streams from both anterior cerebrals and the intraneurysmal flow is

additionally affected by the asymmetry of flow in the efferent A2 segments of the anterior cerebrals.[19,92] Basilar sidewall aneurysms may be affected by the asymmetry of flow distribution in the vertebrals, but the effect of this asymmetry is generally resolved in the length of the basilar artery by the time flow reaches basilar bifurcation aneurysms.[19] Being under the influence of pulsatile flow, these aneurysmal patterns have a temporal quality so that, for example, portions of the fluid in the parent vessel can be driven into the aneurysm vortex during systole and then be distributed either into stagnation zones at the aneurysm dome or into the central vortical regions, while a greater portion (greater as compared to systole) of the intraneurysmal fluid exits the aneurysm during diastole.[53,107] The location near the distal neck where the flow impinges the aneurysm wall and the proportion of the neck area carrying flow into the aneurysm can vary during the cardiac cycle[54,180] and stable or oscillating vortical structures may persist throughout the cardiac cycle or they may be transient, existing only for parts of the cardiac cycle.[67,159] The flow in the parent vessel at the aneurysm neck is also generally disturbed (by the inflow and the outflow) and may contain portions of the intra-aneurysmal vortex, secondary flow structures including helical flow patterns, and recirculation zones.[110,135] Overall, the flow patterns in any given aneurysm in a patient are unique to that aneurysm because the geometry of the aneurysm-parent vessel complex and the parent vessel flow rates are unique to that aneurysm.

There is no difference in intraneurysmal and systemic pulsatile pressure as shown in 34 in vivo aneurysms,[130,157] in 8 patients intra-operatively[38] and endovascularly[41], and in in vitro sidewall aneurysms.[53] There are in vivo experiments suggesting that pressures at the aneurysm dome are statistically lower (mean pressure lower by 10 mmHg in 5 cases,[1] systolic and diastolic lower by 6 mmHg in 80 cases[60]) than systemic values, but the relative magnitude (5–15%) of these differences may have been effected by the recording methods. The augmentation index (ratio of reflected and primary amplitudes in the pressure waveform) at the carotid artery was 8% higher (statistically significant) in aneurysm patients as compared to controls; the index was recorded post-hemorrhage in 90% of the patients at least 2 months after the event,[190] but the effect of the hemorrhage on the difference needs to be investigated. Thus, the significance of pressure vis-à-vis aneurysm pathophysiology is manifested via the stress generated in the diseased arterial segment (i.e., the aneurysm) and the extent to which such stresses are sustainable by the progressively diseased wall.

Classification of Aneurysms and Wall Shear Stress

The quantification of aneurysmal velocities is largely driven by the goal of obtaining wall shear stress (WSS) values at the luminal surface of aneurysms (Figure 4). Intraneurysmal velocities are broadly about an order of magnitude lower than in the parent artery. In idealized aneurysms, velocites are suggested to be proportional to neck area and inversely proportional to the square of the maximum aneurysm diameter, with peak WSS values equaling those at arterial bifurcations (~50–150 dynes/cm^2).[108,168] The flow patterns described above provide a picture of the relative velocities and WSS values in the aneurysm; regions near the neck that acts as a flow divider or regions in the aneurysm body where flow impinges have higher velocity and WSS values while regions where secondary flow structures prevail or regions of flow stagnation have lower velocity and WSS values. Peak velocities ranging from 10% to 150% of the velocity (axial or average) in the parent artery,[10,60,63,108,110,182,183,192] maximal WSS values ranging from 10–1500 dynes/sq.cm,[15,18–20,25,54,63,79,101,110,178] and cardiac cycle-averaged WSS values ranging from 10–220 dynes/sq.cm[13,55,171,178,179] have been reported. Minimum values of velocities and WSS are, in general, in the sub-decimal range in almost all studies. WSS has been inversely related to the aspect ratio,[161,211] dome diameter,[181] and the surface area[79] of aneurysms and low WSS and increased residence times are correlated to thrombosis.[144] Regardless of the value of the WSS or the method of its evaluation, it is important to emphasize that it is not

only a difficult variable to evaluate with high fidelity but that the calculated values only represent a snapshot in the lifetime of an aneurysm.

Technological progress has enabled the development of sophisticated algorithms to extract surface geometries from patient medical imaging data that facilitate numerical simulations on geometries that are 'patient-specific'.[3,22,27,63,139] Such developments allow for numerical calculations of flow fields in the entire circle of Willis[2] or correlations of global morphological and hemodynamic variables to incidence and rupture patterns;[132] the latter study finds tapers in the internal carotid artery to be associated with unruptured aneurysms while greater curvatures of the carotid siphon seem to be a deterrent to aneurysm formation. The ability to perform these numerical simulations with relative ease has also facilitated parametric studies where engineered arterial and aneurysmal geometries can be systematically varied to compare flow patterns and intraneurysmal velocities or where flow patterns can be calculated in several patient-derived geometries; attempts can then be made to extrapolate such results to classify patient morphologies according to hemodynamic patterns. Results include a negative correlation between dome size and intraneurysmal flow velocity,[181] a correlation between aneurysm size at rupture and the diameter of associated side branches,[62] greater flow activity in aneurysms on the outer curvature of arteries and invariance of velocities at the neck with changing aneurysm aspect ratio,[131,155] greater vorticity with decreasing alignment of the aneurysm height to inflow direction,[177] consideration of secondary flow structures in parent vessels with varying tortuosity affecting aneurysmal inflow,[70] secondary vortices/recirculation in terminus aneurysms only when the necks are eccentric to the parent vessel axis and when the eccentricity is less than the parent vessel diameter,[129] identification of a certain threshold of the angular displacement of the aneurysm center to the parent artery axis in one terminus aneurysm resulting in deeper jet penetrance and changed flow structure,[44] increasing complexity of flow patterns and increasing proportion of aneurysmal surface exposed to low (<5 dynes/cm^2) WSS with increasing size ratio.[188]

Cycle-averaged WSS values are found to be inversely proportional to aneurysmal growth displacement;[13] 20–30% of the surface area at the dome of ruptured aneurysms is exposed to low WSS (<4 dynes/cm^2) as compared to 5–10% of the area in unruptured aneurysms;[55,79] the minimum WSS in the group of ruptured aneurysms was found to be half (absolute value 0.2 dynes/cm^2) of the unruptured group in 50 posterior communicating artery aneurysms, but no differences were found in 50 middle cerebral artery aneurysms;[178] areas of low WSS were not significantly different between ruptured and unruptured groups in one study.[25] The maximum WSS (absolute mean ~500 dynes/cm^2) in ruptured aneurysms was found to be significantly higher than that in unruptured aneurysms; other studies support the notion of higher maximal WSS in the ruptured group with[161] and without[79,178] statistical significance. An index of oscillation of the WSS was not significantly different between ruptured and unruptured groups in one study.[178] Ruptured aneurysms were found to more frequently have complex and unstable flow patterns with concentrated inflow regions and smaller impingement zones as compared to unruptured aneurysms.[23,24]

In vitro and numerical studies have evaluated the WSS at arterial regions where aneurysms or bleb regions within aneurysms form by either artificially removing the blebs and aneurysms from geometries obtained post-formation[26,54,118,160] or from geometries obtained pre-and post-formation.[101,179,182,183] The results seem to consistently suggest that blood impinges at a location close to where the neck of the aneurysm or bleb forms with associated high and oscillating WSS (or WSS gradient) values while the region spanned by the neck of the future structure experiences flow recirculation or secondary flow with associated low and oscillating WSS values. After the blebs or aneurysms form, the WSS in these regions drops. Figure 4 shows one such aneurysm where the inflow impinges at the

location where the bleb neck gains definition (high WSS), but a recirculation region that gains vortical structure (lower WSS) exists across the span of the bleb.[183] A range of about 20–200 dynes/cm^2 for peak WSS[26,54,183] and 400–600 dynes/cm^2/mm for spatial WSS gradients[101] have been reported at the pre-aneurysm/pre-bleb edges, minimum WSS values in growth regions are generally close to zero. An oscillatory index of the spatial gradient of the WSS has been associated with the location of aneurysm formation.[160] These results are from a total of 32 cases only and the study with largest sample size (20 cases)[26] states that 20% of blebs were not found at regions with the highest WSS, so additional data are needed to confirm this phenomenon. It is plausible that the search for the cause of aneurysm growth and rupture will require incorporation of the biology, and cannot depend solely on the physics of the flow and its derivative variables in the aneurysm.

Most studies use Newtonian fluid properties for ease of computation or experimentation, but blood is non-Newtonian with shear thinning properties. The non-Newtonian effect is mostly negligible in the parent vessel and near the aneurysm neck, but is much more apparent in low velocity regions.[42,108,134,210] Experiments with non-Newtonian fluids report lower intraneurysmal velocities, weaker vortical structures, more stable and symmetric vortical structures, wider areas of low WSS, and displacement of low WSS regions as compared to Newtonian fluids.[11,42,134,196] WSS values can be 20–50% lower than the lowest values predicted by Newtonian fluids in the low shear rate regions at aneurysm domes, while spatially averaged WSS over the dome regions are about 10–25% lower.[42,196,210] The error with the Newtonian assumption seems to be appreciable when the shear rate is below 10–15 s^{-1} (WSS is less than ~1 dynes/cm^2).[42,210]

Numerical Simulations and Limitations

Numerical simulations are sensitive to the boundary conditions used for the calculations. For example, replacing the vasculature proximal to aneurysms with a straight pipe substantially reduced the impingement and high WSS values (differences of as much as 100–125 dynes/cm^2 at some locations) in the inflow zone.[18] Recordings of flow waveforms in the internal carotid and vertebrobasilar arteries in 39 healthy subjects have suggested that an archetypal waveform for each artery could be constructed and then scaled to the average flow rate in the artery of a specific patient.[43,57] While such waveforms facilitate simulations when flow data from the individual patient are unavailable or they can be used to compare results across various geometries depending on study aims, the accuracy of the results generated with such idealized waveforms can be low if the goal is to quantify the hemodynamics in a specific aneurysm. The cycle-averaged WSS can differ as much as 40 dynes/cm^2 between results from idealized and patient-derived waveforms;[86] altering the flow ratios in the A1 segments by ~35% and 100% can change spatially-averaged WSS by 40% and time-averaged WSS by 100%, respectively.[87,201] Phase-contrast magnetic resonance imaging is becoming the standard mode of measuring flow waveforms in patients due to its non-invasiveness, but measurement of flow waveforms at all inlet and outlet sections of the vascular segment of interest are not yet practicable. Traditional outlet boundary conditions include constant zero pressure (the easiest to implement and the least accurate) and three-component (2 resistances and 1 capacitance) Windkessel, but several others exist;[56,202] differences of 50–70% in the time-averaged WSS have been reported with different boundary conditions.[119,143] Validation studies of numerical simulations with particle image and/or laser Doppler velocimetry and correlations with phase-contrast magnetic resonance imaging in patients have been conducted.[45,66,198] Gross flow structures are generally in agreement in such studies, with any quantitative differences between the numerical and in vitro studies mostly being due to geometry; substantial quantitative differences between the phase-contrast and numerical/in-vitro results can be found due to the lower spatio-temporal resolution of phase-contrast imaging.

Although the assumptions and limitations of numerical simulations are recognized, a couple of cautionary notes may need to be mentioned. All commercially available CFD codes and many of the homegrown codes are based on the Navier Stokes equations that merely describe the second law of Newton, and which are based on continuum mechanics. Blood, of course, is a complicated suspension of formed elements that are deformable and which react not only with each other but also with their surroundings. This interaction is not limited to only physical mechanics, but also biochemical interactions (cellular, molecular, genetic factors referred to in the introduction section). Unfortunately, the laws that govern such biological reactions have not been fully elucidated and thus cannot easily be incorporated into a computational scheme.

The term ‘patient specific’ has been often used in the titles and descriptions of reported simulation results. Although the term is applied loosely and is generally understood to mean ‘patient derived’, some caveats to the implication that the results are specific to the patient may be noted because these limitations also affect the use of these numerical results to explain causative mechanisms of aneurysm pathophysiology. As mentioned previously, since the late seventies, imaging and computer visualization of blood vessels has improved significantly so that three dimensional representations of the lumen of sections of the vascular tree are readily transferrable as structural meshes on which detailed flow calculations can be performed. Since in most cases the vascular wall geometry and mechanical properties are unknown, the common no slip boundary condition is applied. Unfortunately, even with the most up to date imaging equipment, small blood vessels that may branch off larger vessels cannot be visualized, the vasa vasorum[72,97] is invisible (possibly effecting accuracy of near-wall flow calculations) and the exact location of the boundary of the visible vessels themselves is uncertain, requiring a generally arbitrary threshold and smoothening algorithm to prevent the CFD program from encountering badly deformed elements. Additionally, to start the iterative calculations of the flow field within, entry and exit flow conditions into the region of interest are required. The inlet and outlet conditions are not obtained from the individual patient in most studies thus far. Finally, the obtained geometry is a snapshot in time and space and usually it undergoes geometrical changes; the inlet/outlet conditions also change depending on an individual’s posture and level of activity. Another cautionary note is with regards to the pressure fields generated by CFD simulations and the extrapolation of changes in pressure within the computational domain to the biological system. It is well accepted that CFD can produce physiologically relevant flow rates and flow velocities by simply imposing inlet flow conditions and zero pressure at the outlet(s). The CFD software then seeks iteratively to establish the pressure field that will drive fluid through the computational domain at the imposed inlet mass flow rate and distribute it throughout the region of interest. Imposing zero pressure at the outlet is justified by the fact that regardless of the absolute pressure at the outlet, the pressure gradient between the inlet and outlet remains the same. This is due to the fact that the pressure gradient only needs to overcome mainly viscous dissipation and some fluid inertia. However, in the circulatory system the boundaries that surround the blood do react to its presence in a viscoelastic fashion. Rapid pulsatile pressure changes are transmitted to the surrounding walls which work in harmony with the heart to absorb these rapid pressure changes and attenuate sharp pressure spikes. This is the well-known Windkessel effect and mathematically it is manifested as a substantial reduction in the wave propagation speed as compared to its value inside rigid boundaries. Thus, in a rigid domain all the energy produced by the heart is transmitted to the fluid whereas inside a viscoelastic domain, part of the energy is transmitted to the walls and retransmitted to the fluid in a delayed fashion. Therefore, the pressure flow relationship in the viscoelastic domain is vastly different than in the rigid domain both in terms of absolute changes in pressure values as well as in its phasic relations to the flow wave.

As the kinetic energy of flow impinges on the apices of bifurcations, it is converted to increased pressure and this increase has been speculated (especially from numerical simulations where only the requisite pressure gradient is used to impart flow) to be a factor in aneurysm pathophysiology,[39,47] but consideration of the total pressure at these regions suggests that this pressure increase in only about 2–4% and is unlikely to have any substantial effect.[106,162] There have been suggestions that turbulent flow regimes exist in aneurysms,[39,40,60,148,194] which can drastically effect shear rates and accelerate wall degeneration, but it is much more likely that the recorded phenomena are due to highly disturbed or unstable flow patterns interacting with aneurysm wall fluctuations and not characteristic turbulence[61,71,168,175,192] (characteristics of turbulence include disorder, irreproducibility in detail, efficient mixing and transport, and irregularly distributed three-dimensional vorticity over a wide range of length scales[172]). In other words, such flow patterns may be a probabilistic phenomenon exhibiting complex laminar/transitional structures, and can neither be properly characterized as laminar flow (a deterministic phenomenon) nor as turbulent flow (a stochastic phenomenon). Large discrepancies in CFD results produced by various laboratories, especially in the transitional flow regime, were noted in a validation and verification study conducted by the Food and Drug Administration.[173] Transitional flow and other limiting assumptions (specificity of 'patient-specific' data, blood homogeneity, Newtonian properties, non-compliant walls) in numerical simulations noted above have been addressed before.[170] The overall clinical utility of CFD has also been discussed previously.[21,83,149]

Wall Structure

Histopathological and/or immunohistochemical evaluations of the walls of human cerebral aneurysms suggest that the walls of aneurysms can be differentiated into what are possibly different stages of progression to eventual rupture (Figure 5).[48,49,176,189] Results from three studies[48,90,176] assessing a total of 74 unruptured and 108 ruptured aneurysms suggest that nascent or initial stage aneurysms seem to have their inner surfaces completely covered with endothelial cells with thin 'smooth' walls comprised of linearly organized smooth muscle cells, regular layers of collagen and very little evidence of inflammation. The wall subsequently degrades through two different observed types. The wall thickens, being comprised of fibroblasts and disorganized smooth muscle cells (intimal hyperplasia), but eventually starts to lose its gross 'regularity' and becomes hypocellular showing increased collagen content, and organizing luminal thrombosis. In what can be considered the final stage before rupture, the wall becomes irregular, extremely thin, and hypocellular with obscure layers of collagen and sparse smooth muscle cells. Ruptured aneurysm walls were mostly comprised of an acellular proteinacious structure (hyaline-like) with sparse smooth muscle cells and irregular collagenous layers with diffuse infiltration of macrophages and leukocytes. It may be noted that the temporal nature of degradation through these four wall types is only an inference based on literature evidence. Also the entire aneurysm wall does not necessarily delineate itself into these wall types; degeneration of the wall increases from the neck to the dome[189] and aneurysm ruptures mostly (80–85% of cases[30,31]) occur at the dome.

In comparison to peripheral arterial walls, cerebral arterial walls have negligible elastin in the medial and adventitial layers with no external elastic lamina, which makes cerebral arteries much stiffer (less distensible) than peripheral arteries.[39,65,124] Aneurysm wall thickness can range from 15 to 700 microns;[29,112] the anisotropy induced by collagen in the aneurysm wall has been measured;[112] the yield to breaking strength of aneurysm wall tissue seems to be around 0.5–2 MPa;[112,167] uniaxial tests of meridional strips of aneurysm tissue suggest a best-fit to a three-parameter Mooney-Rivlin model and show a statistical (n=16) difference in one of the model parameters between ruptured and unruptured aneurysms;[29]

biaxial tests with best-fit Hookean and two-parameter Mooney Rivlin model parameters have been published.[187] The pulsatile motion of some aneurysm walls has been imaged[64,85] (average displacements of 40–300 microns are reported[85]), but currently achievable spatio-temporal resolution can substantially effect accuracy. Further, attempts are being made to use such wall motion behavior to estimate the unknown material properties of the aneurysm wall through inverse analysis schemes.[6,99,214] Numerical schemes are also being developed to simulate wall remodeling (mostly by simulating collagen turnover) and growth of aneurysms.[37,68,100,203]

Early suggestions that volume distension (ballooning) of aneurysm walls or mechanical fatigue made severe by resonant fluctuations can substantially contribute to aneurysm growth and rupture[58,123] do not seem to be valid.[32,69,174,175,193] As smooth muscle cells in the medial layer are arranged circumferentially, there is a gap in the medial layer at the apices of bifurcations and this gap had been thought of as a weak point predisposed to aneurysm formation, but the fact that this region has abundant collagen fibers running along the gap,[16] that these gaps occur in at least 60% to 100% of all bifurcations[16,52,205] (while aneurysms occur in 5% of patients), and that ex vivo pressures of 600 mmHg do not expose these spots as weak[52] make these gaps unlikely to be a substantial factor. Due to the shear stress environment[215] at bifurcation apices, these regions tend to develop a cushion/pad-like region of intimal thickening over time (incidence ~20% by age 10 years, ~60% in adults[205]) that can project into the lumen. Although an ex-vivo steady flow study in rodent bifurcations suggests that flow stagnation exists distal to these intimal pads,[127] it is unclear if these can cause flow separation and substantially affect aneurysm initiation in patients; these structures are also widely prevalent at human bifurcations (at >60% of bifurcations[205]), which, again, does not match aneurysm prevalence.

Numerical simulations that incorporate deformable wall properties with pulsatile blood flow (called fluid-structure interaction, FSI) in artificial and patient-derived aneurysm geometries have also been carried out.[5,110,184,185,195] In general, the use of deformable walls does not affect the gross flow patterns, but the secondary flow structures can be different with lower peak velocities and WSS values. In zones of low/stagnant flow, wall compliance can increase the minimal velocities (and minimal WSS).[110,186] Maximal aneurysm wall displacements ranging from 150 to 750 microns,[7,185,186,195] percent reduction in maximal WSS due to deformable walls (as compared to rigid) ranging from 10–35%,[7,8,186] and maximal wall stress at the dome of around 0.2–0.3 MPa[5,7,8,195] are reported. Assuming a uniform wall thickness (300 microns) can reduce the maximal wall displacement by 40–45% and increase the spatially averaged systolic WSS by 60–90% as compared to an assumption of physiological variation in the wall thickness (300 microns at parent vessel to 50 microns at the dome).[185]

Summary and Hypothesis

The hemodynamics of cerebral aneurysms has been reviewed before.[75,103,133,158,159,209] The impetus of all the studies mentioned above can be categorized into one broad and one specific goal. The global goal is to identify physical mechanisms that are responsible for aneurysm pathophysiology and the more specific goal is the prognosis of a given (usually unruptured) aneurysm using these physical variables. The abundance of studies investigating variations in morphological and hemodynamic (and combinations of morphological and hemodynamic) parameters may facilitate achievement of the latter goal, but in general this seems far away. The prognostic relevance of these parameters has been questioned[209] and, at the least, much larger sample sizes and multivariate analyses are required to distil predictive values. Aside from the assumptions made in numerical studies (which could be overcome with technological advancement), the biggest hurdle is that the predictive value of

such studies may remain limited until biochemical degradation of the aneurysmal wall can be simulated and incorporated.[113,122] Ever more sophisticated computations incorporating the entire circle of Willis, pulsatile flow, wall deformability, and wall degeneration leading to aneurysm growth are being developed.[35] It is plausible, however, that advancements in medical imaging of flow in intracranial aneurysms[74,199] or of the aneurysmal wall[117,140] in individual patients will, in the near future, provide greater predictive values and obviate the need for simulations in this regard.

In terms of physical mechanisms facilitating aneurysm pathophysiology, it is clear that no geometrical factor(s) currently exists to classify aneurysms according to rupture status, no inherent anomalies in the circle of Willis clearly delineate the propensity of the vasculature to form aneurysms or to cause aneurysm rupture, and no hemodynamic discriminant (only WSS or its derivatives have really been evaluated) is currently able to predict aneurysm formation, growth or rupture. Some guidelines can, however, be gathered from the collected evidence. The results of these studies suggest that complex (or separated or recirculating or secondary or disturbed or unstable or oscillating) flow structures are involved in the growth and rupture of aneurysms and that the growth of aneurysms occurs at low flow (or slow or stagnant or low shear) regions. It is also sufficiently clear that aneurysm rupture occurs at the dome (at the dome of aneurysms or at the dome of blebs that may form on the aneurysm body). The current, generally accepted, hypothesis is that the initiation of aneurysms is related to (mechanical) degeneration of the bifurcation apex due to the high shear stress or high shear stress gradient in this region. Data also suggest that the initial location of aneurysms is distal to the bifurcation apices where shear gradient zones would be higher.[120,153,189] In vivo experiments have certainly demonstrated that artificially creating a high(er) hemodynamic stress environment at bifurcations leads to apparent degenerative changes in the elastic lamina near the apices with lesions resembling incipient aneurysms.[93,95,121,165] To match the prevalence of aneurysms, this mechanism should reasonably imply that the shear stress at the middle cerebral artery bifurcation (~20% of aneurysms), the anterior cerebral-anterior communicating artery junction (~30%), and the internal carotid-posterior communicating artery junction (~25%) should be higher than that at the basilar or internal carotid bifurcations. Peak systolic velocities in the middle cerebral artery seem to be at least 30–50% higher than those in the basilar artery, but further evaluation is required to quantify the shear stress differences at these locations.

Another plausible physical mechanism that may contribute to aneurysm initiation is the fact that the stagnation point at the bifurcation apices (or within aneurysms) migrates at different parent artery flow rates.[101,191,211] The movement due to pulsatile flow is further exaggerated by heart-rate variability (60% variation in mean middle cerebral artery velocity has been noted[200]). This constant stochastic migration of the impingement point within a small area, or spot, subjects the endothelial cells to frequent changes in the shear direction and can facilitate the initiation of aneurysms. Heart rate variability and stagnation spots are yet to be evaluated in detail, but two previous experiments[77,197] clearly show the effect that vibration (an equivalent phenomenon) can have on transitional flows. It is thus plausible that one of the three indices of oscillatory shear stress that have been developed to correlate with aneurysm initiation,[118,160] or another such index, correlates better with locations of aneurysm initiation rather than just high WSS or WSS gradients. Further evaluation is needed to verify this mechanism. Hemodynamic factors may be correlated to the distribution of aneurysms within the circle of Willis, but all such mechanistic explanations will probably only serve as necessary but not sufficient causative conditions of aneurysm pathophysiology.

References

1. Acar F, Men S, Tayfur V, Yilmaz O, Erbayraktar S, Metin Güner E. In vivo intraaneurysmal pressure measurements in experimental lateral wall aneurysms before and after onyx embolization. Surg Neurol. 2006; 66:252–256. [PubMed: 16935627]
2. Alnaes MS, Isaksen J, Mardal KA, Romner B, Morgan MK, Ingebrigtsen T. Computation of hemodynamics in the circle of Willis. Stroke. 2007; 38:2500–2505. [PubMed: 17673714]
3. Antiga L, Piccinelli M, Botti L, Ene-Iordache B, Remuzzi A, Steinman DA. An image-based modeling framework for patient-specific computational hemodynamics. Medical & Biological Engineering & Computing. 2008; 46:1097–1112. [PubMed: 19002516]
4. Baharoglu MI, Lauric A, Gao BL, Malek AM. Identification of a dichotomy in morphological predictors of rupture status between sidewall- and bifurcation-type intracranial aneurysms. J Neurosurg. 2012; 116:871–881. [PubMed: 22242668]
5. Bai-Nan X, Fu-Yu W, Lei L, Xiao-Jun Z, Hai-Yue J. Hemodynamics model of fluid-solid interaction in internal carotid artery aneurysms. Neurosurg Rev. 2011; 34:39–47. [PubMed: 20812022]
6. Balocco S, Camara O, Vivas E, Sola T, Guimaraens L, Gratama van Andel HA, Majoie CB, Pozo JM, Bijnens BH, Frangi AF. Feasibility of estimating regional mechanical properties of cerebral aneurysms in vivo. Med Phys. 2010; 37:1689–1706. [PubMed: 20443490]
7. Bazilevs Y, Hsu MC, Zhang Y, Wang W, Liang X, Kvamsdal T, Brekken R, Isaksen JG. A fully-coupled fluid-structure interaction simulation of cerebral aneurysms. Computational Mechanics. 2010; 46:3–16.
8. Bazilevs Y, Hsu MC, Zhang Y, Wang W, Kvamsdal T, Hentschel S, Isaksen JG. Computational vascular fluid-structure interaction: methodology and application to cerebral aneurysms. Biomech Model Mechanobiol. 2010; 9:481–498. [PubMed: 20111978]
9. Beck J, Rohde S, Berkefeld J, Seifert V, Raabe A. Size and location of ruptured and unruptured intracranial aneurysms measured by 3-dimensional rotational angiography. Surg Neurol. 2006; 65:18–25. [PubMed: 16378842]
10. Benndorf G, Wellnhofer E, Lanksch W, Felix R. Intraaneurysmal flow: evaluation with Doppler guidewires. AJNR Am J Neuroradiol. 1996; 17:1333–1337. [PubMed: 8871720]
11. Bernsdorf J, Wang D. Non-Newtonian blood flow simulation in cerebral aneurysms. Computers and Mathematics with Applications. 2009; 58:1024–1029.
12. Bor AS, Velthuis BK, Majoie CB, Rinkel GJ. Configuration of intracranial arteries and development of aneurysms: a follow-up study. Neurology. 2008; 70:700–705. [PubMed: 18299521]
13. Boussel L, Rayz V, McCulloch C, Martin A, Acevedo-Bolton G, Lawton M, Higashida R, Smith WS, Young WL, Saloner D. Aneurysm growth occurs at region of low wall shear stress: patient-specific correlation of hemodynamics and growth in a longitudinal study. Stroke. 2008; 39:2997–3002. [PubMed: 18688012]
14. Brisman JL, Song JK, Newell DW. Cerebral aneurysms. N Engl J Med. 2006; 355:928–939. [PubMed: 16943405]
15. Burleson AC, Strother CM, Turitto VT. Computer modeling of intracranial saccular and lateral aneurysms for the study of their hemodynamics. Neurosurgery. 1995; 37:774–782. [PubMed: 8559308]
16. Canham PB, Finlay HM. Morphometry of medial gaps of human brain artery branches. Stroke. 2004; 35:1153–1157. [PubMed: 15017007]
17. Carter BS, Sheth S, Chang E, Sethl M, Ogilvy CS. Epidemiology of the size distribution of intracranial bifurcation aneurysms: smaller size of distal aneurysms and increasing size of unruptured aneurysms with age. Neurosurgery. 2006; 58:217–223. [PubMed: 16462474]
18. Castro MA, Putman CM, Cebral JR. Computational fluid dynamics modeling of intracranial aneurysms: effects of parent artery segmentation on intra-aneurysmal hemodynamics. AJNR Am J Neuroradiol. 2006; 27:1703–1709. [PubMed: 16971618]

19. Castro MA, Putman CM, Cebral JR. Patient-specific computational modeling of cerebral aneurysms with multiple avenues of flow from 3D rotational angiography images. Acad Radiol. 2006; 13:811–821. [PubMed: 16777554]
20. Castro MA, Putman CM, Sheridan MJ, Cebral JR. Hemodynamic patterns of anterior communicating artery aneurysms: a possible association with rupture. AJNR Am J Neuroradiol. 2009; 30:297–302. [PubMed: 19131411]
21. Cebral JR, Meng H. Counterpoint: realizing the clinical utility of computational fluid dynamics--closing the gap. AJNR Am J Neuroradiol. 2012; 33:396–398. [PubMed: 22282452]
22. Cebral JR, Castro MA, Appanaboyina S, Putman CM, Millan D, Frangi AF. Efficient pipeline for image-based patient-specific analysis of cerebral aneurysm hemodynamics: technique and sensitivity. IEEE Trans Med Imaging. 2005; 24:457–467. [PubMed: 15822804]
23. Cebral JR, Castro MA, Burgess JE, Pergolizzi RS, Sheridan MJ, Putman CM. Characterization of cerebral aneurysms for assessing risk of rupture by using patient-specific computational hemodynamics models. AJNR Am J Neuroradiol. 2005; 26:2550–2559. [PubMed: 16286400]
24. Cebral JR, Mut F, Weir J, Putman CM. Association of hemodynamic characteristics and cerebral aneurysm rupture. AJNR Am J Neuroradiol. 2011; 32:264–270. [PubMed: 21051508]
25. Cebral JR, Mut F, Weir J, Putman CM. Quantitative characterization of the hemodynamic environment in ruptured and unruptured brain aneurysms. AJNR Am J Neuroradiol. 2011; 32:145–151. [PubMed: 21127144]
26. Cebral JR, Sheridan M, Putman CM. Hemodynamics and bleb formation in intracranial aneurysms. AJNR Am J Neuroradiol. 2010; 31:304–310. [PubMed: 19797790]
27. Chang HH, Duckwiler GR, Valentine DJ, Chu WC. Computer-assisted extraction of intracranial aneurysms on 3D rotational angiograms for computational fluid dynamics modeling. Medical Physics. 2009; 36:5612–5621. [PubMed: 20095274]
28. Chyatte D, Lewis I. Gelatinase activity and the occurrence of cerebral aneurysms. Stroke. 1997; 28:799–804. [PubMed: 9099199]
29. Costalat V, Sanchez M, Ambard D, Thines L, Lonjon N, Nicoud F, Brunel H, Lejeune JP, Dufour H, Bouillot P, Lhaldky JP, Kouri K, Segnarbieux F, Maurage CA, Lobotesis K, Villa-Uriol MC, Zhang C, Frangi AF, Mercier G, Bonafé A, Sarry L, Jourdan F. Biomechanical wall properties of human intracranial aneurysms resected following surgical clipping (IRRAs Project). J Biomech. 2011; 44:2685–2691. [PubMed: 21924427]
30. Crawford T. Some observations on the pathogenesis and natural history of intracranial aneurysms. J Neurol Neurosurg Psychiatry. 1959; 22:259–266. [PubMed: 13812726]
31. Crompton MR. Mechanism of growth and rupture in cerebral berry aneurysms. Br Med J. 1966; 1:1138–1142. [PubMed: 5932074]
32. David G, Humphrey JD. Further evidence for the dynamic stability of intracranial saccular aneurysms. J Biomech. 2003; 36:1143–1150. [PubMed: 12831740]
33. de Rooij NK, Linn FH, van der Plas JA, Algra A, Rinkel GJ. Incidence of subarachnoid haemorrhage: a systematic review with emphasis on region, age, gender and time trends. J Neurol Neurosurg Psychiatry. 2007; 78:1365–1372. [PubMed: 17470467]
34. de Rooij NK, Velthuis BK, Algra A, Rinkel GJ. Configuration of the circle of Willis, direction of flow, and shape of the aneurysm as risk factors for rupture of intracranial aneurysms. J Neurol. 2009; 256:45–50. [PubMed: 19221852]
35. Di Achille P, Humphrey JD. Toward large-scale computational fluid-solid-growth models of intracranial aneurysms. Yale Journal of Biology & Medicine. 2012; 85:217–228. [PubMed: 22737050]
36. Feigin VL, Rinkel GJ, Lawes CM, Algra A, Bennett DA, van Gijn J, Anderson CS. Risk factors for subarachnoid hemorrhage: an updated systematic review of epidemiological studies. Stroke. 2005; 36:2773–2780. [PubMed: 16282541]
37. Feng Y, Wada S, Tsubota K, Yamaguchi T. The application of computer simulation in the genesis and development of intracranial aneurysms. Technol Health Care. 2005; 13:281–291. [PubMed: 16055976]
38. Ferguson GG. Direct measurement of mean and pulsatile blood pressure at operation in human intracranial saccular aneurysms. J Neurosurg. 1972; 36:560–563. [PubMed: 5026542]

39. Ferguson GG. Physical factors in the initiation, growth, and rupture of human intracranial saccular aneurysms. J Neurosurg. 1972; 37:666–677. [PubMed: 4654696]
40. Ferguson GG. Turbulence in human intracranial saccular aneurysms. J Neurosurg. 1970; 33:485–497. [PubMed: 5479489]
41. Ferns SP, Schneiders JJ, Siebes M, van den Berg R, van Bavel ET, Majoie CB. Intracranial blood-flow velocity and pressure measurements using an intra-arterial dual-sensor guidewire. AJNR Am J Neuroradiol. 2010; 31:324–326. [PubMed: 19762460]
42. Fisher C, Rossmann JS. Effect of non-newtonian behavior on hemodynamics of cerebral aneurysms. J Biomech Eng. 2009; 131:091004. [PubMed: 19725693]
43. Ford MD, Alperin N, Lee SH, Holdsworth DW, Steinman DA. Characterization of volumetric flow rate waveforms in the normal internal carotid and vertebral arteries. Physiol Meas. 2005; 26:477–488. [PubMed: 15886442]
44. Ford MD, Lee SW, Lownie SP, Holdsworth DW, Steinman DA. On the effect of parent-aneurysm angle on flow patterns in basilar tip aneurysms: towards a surrogate geometric marker of intra-aneurismal hemodynamics. J Biomech. 2008; 41:241–248. [PubMed: 18078944]
45. Ford MD, Nikolov HN, Milner JS, Lownie SP, Demont EM, Kalata W, Loth F, Holdsworth DW, Steinman DA. PIV-measured versus CFD-predicted flow dynamics in anatomically realistic cerebral aneurysm models. J Biomech Eng. 2008; 130:021015. [PubMed: 18412502]
46. Forget TR Jr, Benitez R, Veznedaroglu E, Sharan A, Mitchell W, Silva M, Rosenwasser RH. A review of size and location of ruptured intracranial aneurysms. Neurosurgery. 2001; 49:1322–1325. [PubMed: 11846931]
47. Foutrakis GN, Yonas H, Sclabassi RJ. Saccular aneurysm formation in curved and bifurcating arteries. AJNR Am J Neuroradiol. 1999; 20:1309–1317. [PubMed: 10472991]
48. Frösen J, Piippo A, Paetau A, Kangasniemi M, Niemelä M, Hernesniemi J, Jaaskelainen J. Remodeling of saccular cerebral artery aneurysm wall is associated with rupture: histological analysis of 24 unruptured and 42 ruptured cases. Stroke. 2004; 35:2287–2293. [PubMed: 15322297]
49. Frösen J, Tulamo R, Paetau A, Laaksamo E, Korja M, Laakso A, Niemelä M, Hernesniemi J. Saccular intracranial aneurysm: pathology and mechanisms. Acta Neuropathol. 2012; 123:773–786. [PubMed: 22249619]
50. Gambaruto AM, João AJ. Flow structures in cerebral aneurysms. Computers and Fluids. 2012; 65:56–65.
51. German WJ, Black SP. Intra-aneurysmal hemodynamics-jet action. Circ Res. 1955; 3:463–468. [PubMed: 13250713]
52. Glynn LE. Medial defects in the circle of Willis and their relation to aneurysm formation. The Journal of Pathology and Bacteriology. 1940; 51:213–222.
53. Gobin YP, Counord JL, Flaud P, Duffaux J. In vitro study of haemodynamics in a giant saccular aneurysm model: influence of flow dynamics in the parent vessel and effects of coil embolisation. Neuroradiology. 1994; 36:530–536. [PubMed: 7845578]
54. Gonzalez CF, Cho YI, Ortega HV, Moret J. Intracranial aneurysms: flow analysis of their origin and progression. AJNR Am J Neuroradiol. 1992; 13:181–188. [PubMed: 1595440]
55. Goubergrits L, Schaller J, Kertzscher U, van den Bruck N, Poethkow K, Petz Ch, Hege HC, Spuler A. Statistical wall shear stress maps of ruptured and unruptured middle cerebral artery aneurysms. J R Soc Interface. 2012; 9:677–688. [PubMed: 21957117]
56. Grinberg L, Karniadakis GE. Outflow boundary conditions for arterial networks with multiple outlets. Ann Biomed Eng. 2008; 36:1496–1514. [PubMed: 18612828]
57. Gwilliam MN, Hoggard N, Capener D, Singh P, Marzo A, Verma PK, Wilkinson ID. MR derived volumetric flow rate waveforms at locations within the common carotid, internal carotid, and basilar arteries. J Cereb Blood Flow Metab. 2009; 29:1975–1982. [PubMed: 19756018]
58. Hademenos GJ. The physics of cerebral aneurysms. Physics Today. 1995; 48:24–30.
59. Hademenos GJ, Massoud TF, Turjman F, Sayre JW. Anatomical and morphological factors correlating with rupture of intracranial aneurysms in patients referred for endovascular treatment. Neuroradiology. 1998; 40:755–760. [PubMed: 9860129]

60. Hashimoto T. Flow velocity studies in vein pouch model aneurysms. Neurol Res. 1993; 15:185–191. [PubMed: 8103585]
61. Haslach HW Jr. A nonlinear dynamical mechanism for bruit generation by an intracranial saccular aneurysm. J Math Biol. 2002; 45:441–460. [PubMed: 12424532]
62. Hassan T, Timofeev EV, Saito T, Shimizu H, Ezura M, Matsumoto Y, Takayama K, Tominaga T, Takahashi A. A proposed parent vessel geometry-based categorization of saccular intracranial aneurysms: computational flow dynamics analysis of the risk factors for lesion rupture. J Neurosurg. 2005; 103:662–680. [PubMed: 16266049]
63. Hassan T, Timofeev EV, Saito T, Shimizu H, Ezura M, Tominaga T, Takahashi A, Takayama K. Computational replicas: anatomic reconstructions of cerebral vessels as volume numerical grids at three-dimensional angiography. AJNR Am J Neuroradiol. 2004; 25:1356–1365. [PubMed: 15466332]
64. Hayakawa M, Maeda S, Sadato A, Tanaka T, Kaito T, Hattori N, Ganaha T, Moriya S, Katada K, Murayama K, Kato Y, Hirose Y. Detection of pulsation in ruptured and unruptured cerebral aneurysms by electrocardiographically gated 3-dimensional computed tomographic angiography with a 320-row area detector computed tomography and evaluation of its clinical usefulness. Neurosurgery. 2011; 69:843–851. [PubMed: 21623246]
65. Hayashi K, Handa H, Nagasawa S, Okumura A, Moritake K. Stiffness and elastic behavior of human intracranial and extracranial arteries. J Biomech. 1980; 13:175–184. [PubMed: 7364778]
66. Hollnagel DI, Summers PE, Poulikakos D, Kollias SS. Comparative velocity investigations in cerebral arteries and aneurysms: 3D phase-contrast MR angiography, laser Doppler velocimetry and computational fluid dynamics. NMR Biomed. 2009; 22:795–808. [PubMed: 19412933]
67. Holscher T, Rodriguez-Rodriguez J, Wilkening WG, Lasheras JC, U HS. Intraoperative brain ultrasound: a new approach to study flow dynamics in intracranial aneurysms. Ultrasound in Medicine & Biology. 2006; 32:1307–1313. [PubMed: 16965970]
68. Humphrey JD, Baek S, Rajagopal KR. Competition between radial expansion and thickening in the enlargement of an intracranial saccular aneurysm. Journal of Elasticity. 2005; 80:13–31.
69. Humphrey JD, Kyriacou SK. The use of Laplace's equation in aneurysm mechanics. Neurol Res. 1996; 18:204–208. [PubMed: 8837052]
70. Imai Y, Sato K, Ishikawa T, Yamaguchi T. Inflow into saccular cerebral aneurysms at arterial bends. Ann Biomed Eng. 2008; 36:1489–1495. [PubMed: 18563567]
71. Imbesi SG, Kerber CW. Analysis of slipstream flow in two ruptured intracranial cerebral aneurysms. AJNR Am J Neuroradiol. 1999; 20:1703–1705. [PubMed: 10543644]
72. Inci S, Spetzler RF. Intracranial aneurysms and arterial hypertension: a review and hypothesis. Surg Neurol. 2000; 53:530–540. discussion 540–532. [PubMed: 10940419]
73. Ingebrigtsen T, Morgan MK, Faulder K, Ingebrigtsen L, Sparr T, Schirmer H. Bifurcation geometry and the presence of cerebral artery aneurysms. J Neurosurg. 2004; 101:108–113. [PubMed: 15255260]
74. Isoda H, Ohkura Y, Kosugi T, Hirano M, Takeda H, Hiramatsu H, Yamashita S, Takehara Y, Alley MT, Bammer R, Pelc NJ, Namba H, Sakahara H. In vivo hemodynamic analysis of intracranial aneurysms obtained by magnetic resonance fluid dynamics (MRFD) based on time-resolved three-dimensional phase-contrast MRI. Neuroradiology. 2010; 52:921–928. [PubMed: 20012431]
75. Jeong W, Rhee K. Hemodynamics of cerebral aneurysms: computational analyses of aneurysm progress and treatment. Comput Math Methods Med. 2012:782801. [PubMed: 22454695]
76. Jeong YG, Jung YT, Kim MS, Eun CK, Jang SH. Size and location of ruptured intracranial aneurysms. J Korean Neurosurg Soc. 2009; 45:11–15. [PubMed: 19242565]
77. Jones SA, Fronek A. Effects of vibrations on steady flow downstream of a stenosis. J. Biomechanics. 1988; 21:903–914.
78. Joo SW, Lee SI, Noh SJ, Jeong YG, Kim MS, Jeong YT. What Is the Significance of a Large Number of Ruptured Aneurysms Smaller than 7 mm in Diameter? J Korean Neurosurg Soc. 2009; 45:85–89. [PubMed: 19274117]
79. Jou LD, Lee DH, Morsi H, Mawad ME. Wall shear stress on ruptured and unruptured intracranial aneurysms at the internal carotid artery. AJNR Am J Neuroradiol. 2008; 29:1761–1767. [PubMed: 18599576]

80. Juvela S. Prehemorrhage risk factors for fatal intracranial aneurysm rupture. Stroke. 2003; 34:1852–1857. [PubMed: 12829865]
81. Juvela S, Porras M, Poussa K. Natural history of unruptured intracranial aneurysms: probability and risk factors for aneurysm rupture. Neurosurg Focus. 2000; 8:1–9.
82. Juvela S, Hillbom M, Numminen H, Koskinen P. Cigarette smoking and alcohol consumption as risk factors for aneurysmal subarachnoid hemorrhage. Stroke. 1993; 24:639–646. [PubMed: 8488517]
83. Kallmes DF. Point: CFD--computational fluid dynamics or confounding factor dissemination. AJNR Am J Neuroradiol. 2012; 33:395–396. [PubMed: 22268081]
84. Kapoor K, Singh B, Dewan LI. Variations in the configuration of the circle of Willis. Anat Sci Int. 2008; 83:96–106. [PubMed: 18507619]
85. Karmonik C, Diaz O, Grossman R, Klucznik R. In-vivo quantification of wall motion in cerebral aneurysms from 2D cine phase contrast magnetic resonance images. Rofo. 2010; 182:140–150. [PubMed: 19859863]
86. Karmonik C, Yen C, Diaz O, Klucznik R, Grossman RG, Benndorf G. Temporal variations of wall shear stress parameters in intracranial aneurysms--importance of patient-specific inflow waveforms for CFD calculations. Acta Neurochir (Wien). 2010; 152:1391–1398. [PubMed: 20390310]
87. Karmonik C, Yen C, Grossman RG, Klucznik R, Benndorf G. Intra-aneurysmal flow patterns and wall shear stresses calculated with computational flow dynamics in an anterior communicating artery aneurysm depend on knowledge of patient-specific inflow rates. Acta Neurochir (Wien). 2009; 151:479–485. [PubMed: 19343271]
88. Kassam AB, Horowitz M, Chang YF, Peters D. Altered arterial homeostasis and cerebral aneurysms: a molecular epidemiology study. Neurosurgery. 2004; 54:1450–1460. [PubMed: 15157303]
89. Kasuya H, Shimizu T, Nakaya K, Sasahara A, Hori T, Takakura K. Angles between A1 and A2 segments of the anterior cerebral artery visualized by three-dimensional computed tomographic angiography and association of anterior communicating artery aneurysms. Neurosurgery. 1999; 45:89–93. [PubMed: 10414570]
90. Kataoka K, Taneda M, Asai T, Kinoshita A, Ito M, Kuroda R. Structural fragility inflammatory response of ruptured cerebral aneurysms. A comparative study between ruptured and unruptured cerebral aneurysms. Stroke. 1999; 30:1396–1401. [PubMed: 10390313]
91. Kayembe KN, Sasahara M, Hazama F. Cerebral aneurysms and variations in the circle of Willis. Stroke. 1984; 15:846–850. [PubMed: 6474536]
92. Kerber CW, Imbesi SG, Knox K. Flow dynamics in a lethal anterior communicating artery aneurysm. AJNR Am J Neuroradiol. 1999; 20:2000–2003. [PubMed: 10588134]
93. Kim C, Cervós-Navarro J, Kikuchi H, Hashimoto N, Hazama F. Alterations in cerebral vessels in experimental animals and their possible relationship to the development of aneurysms. Surg Neurol. 1992; 38:331–337. [PubMed: 1485208]
94. Kim SC, Singh M, Huang J, Prestigiacomo CJ, Winfree CJ, Solomon RA, Connolly ES Jr. Matrix metalloproteinase-9 in cerebral aneurysms. Neurosurgery. 1997; 41:642–666. [PubMed: 9310982]
95. Kojima M, Handa H, Hashimoto N, Kim C, Hazama F. Early changes of experimentally induced cerebral aneurysms in rats: scanning electron microscopic study. Stroke. 1986; 17:835–841. [PubMed: 3764951]
96. Krex D, Schackert H, Shackert G. Genesis of Cerbral Aneuryms – An Update. Acta Neurochir (Wien). 2001; 143:429–449. [PubMed: 11482693]
97. Krings T, Piske RL, Lasjaunias PL. Intracranial arterial aneurysm vasculopathies: targeting the outer vessel wall. Neuroradiology. 2005; 47:931–937. [PubMed: 16136262]
98. Krischek B, Inoue I. The genetics of intracranial aneurysms. J Hum Genet. 2006; 51:587–594. [PubMed: 16736093]
99. Kroon M, Holzapfel GA. Estimation of the distributions of anisotropic, elastic properties and wall stresses of saccular cerebral aneurysms by inverse analysis. Proceedings of the Royal Society A: Mathematical, Physical and Engineering Sciences. 2008; 464:807–825.

100. Kroon M, Holzapfel GA. A model for saccular cerebral aneurysm growth by collagen fibre remodelling. J Theor Biol. 2007; 247:775–787. [PubMed: 17482213]
101. Kulcsár Z, Ugron A, Marosfoi M, Berentei Z, Paál G, Szikora I. Hemodynamics of cerebral aneurysm initiation: the role of wall shear stress and spatial wall shear stress gradient. AJNR Am J Neuroradiol. 2011; 32:587–594. [PubMed: 21310860]
102. Lall RR, Eddleman CS, Bendok BR, Batjer HH. Unruptured intracranial aneurysms and the assessment of rupture risk based on anatomical and morphological factors: sifting through the sands of data. Neurosurg Focus. 2009; 26:E2. [PubMed: 19408998]
103. Lasheras JC. The biomechanics of arterial aneurysms. Annual Review of Fluid Mechanics. 2007; 39:293–319.
104. Lauric A, Miller EL, Baharoglu MI, Malek AM. 3D shape analysis of intracranial aneurysms using the writhe number as a discriminant for rupture. Ann Biomed Eng. 2011; 39:1457–1469. [PubMed: 21225345]
105. Lazzaro MA, Ouyang B, Chen M. The role of circle of Willis anomalies in cerebral aneurysm rupture. J Neurointerv Surg. 2012; 4:22–26. [PubMed: 21990452]
106. Lieber BB, Gounis MJ. The physics of endoluminal stenting in the treatment of cerebrovascular aneurysms. Neurol Res. 2002; 24:S33–S42. [PubMed: 12074435]
107. Lieber BB, Stancampiano AP, Wakhloo AK. Alteration of hemodynamics in aneurysm models by stenting: influence of stent porosity. Ann Biomed Eng. 1997; 25:460–469. [PubMed: 9146801]
108. Liepsch DW, Steiger HJ, Poll A, Reulen HJ. Hemodynamic stress in lateral saccular aneurysms. Biorheology. 1987; 24:689–710. [PubMed: 2971404]
109. Longstreth WT Jr, Koepsell TD, Yerby MS, van Belle G. Risk factors for subarachnoid hemorrhage. Stroke. 1985; 16:377–385. [PubMed: 3890278]
110. Low MK, Perktold K, Raunig R. Hemodynamics in rigid and distensible saccular aneurysms: a numerical study of pulsatile flow characteristics. Biorheology. 1993; 30:287–298. [PubMed: 8286729]
111. Ma B, Harbaugh RE, Raghavan ML. Three-dimensional geometrical characterization of cerebral aneurysms. Annals of Biomedical Engineering. 2004; 32:264–273. [PubMed: 15008374]
112. MacDonald DJ, Finlay HM, Canham PB. Directional wall strength in saccular brain aneurysms from polarized light microscopy. Annals of Biomedical Engineering. 2000; 28:533–542. [PubMed: 10925951]
113. Macdonald RL. Dissecting the Complexities of Aneurysm Hemodynamics. World Neurosurg. 2011 Online before print.
114. Macdonald RL. Editorial: on the persisting difficulty of making predictions, especially about the future. J Neurosurg. 2012; 116:866–870. [PubMed: 22242673]
115. Mackenzie JM. The anatomy of aneurysm-bearing circles of Willis. Clin Neuropathol. 1991; 10:187–189. [PubMed: 1884526]
116. Mackey J, Brown RD Jr, Moomaw CJ, Sauerbeck L, Hornung R, Gandhi D, Woo D, Kleindorfer D, Flaherty ML, Meissner I, Anderson C, Connolly ES, Rouleau G, Kallmes DF, Torner J, Huston J 3rd, Broderick JP. Unruptured intracranial aneurysms in the Familial Intracranial Aneurysm and International Study of Unruptured Intracranial Aneurysms cohorts: differences in multiplicity and location. J Neurosurg. 2012; 117:60–64. [PubMed: 22540404]
117. Mahmood U. Science to practice: can an enzyme-sensitive MR contrast agent be used to image inflammation in aneurysms? Radiology. 2009; 252:627–628. [PubMed: 19717746]
118. Mantha A, Karmonik C, Benndorf G, Strother C, Metcalfe R. Hemodynamics in a cerebral artery before and after the formation of an aneurysm. AJNR Am J Neuroradiol. 2006; 27:1113–1118. [PubMed: 16687554]
119. Marzo A, Singh P, Larrabide I, Radaelli A, Coley S, Gwilliam M, Wilkinson ID, Lawford P, Reymond P, Patel U, Frangi A, Hose DR. Computational hemodynamics in cerebral aneurysms: the effects of modeled versus measured boundary conditions. Ann Biomed Eng. 2011; 39:884–896. [PubMed: 20972626]
120. McDonald CA, Korb M. Intracranial aneurysms. Archives of Neurology & Psychiatry. 1939; 42:298–328.

121. Meng H, Wang Z, Hoi Y, Gao L, Metaxa E, Swartz DD, Kolega J. Complex hemodynamics at the apex of an arterial bifurcation induces vascular remodeling resembling cerebral aneurysm initiation. Stroke. 2007; 38:1924–1931. [PubMed: 17495215]
122. Metcalfe RW. The promise of computational fluid dynamics as a tool for delineating therapeutic options in the treatment of aneurysms. AJNR Am J Neuroradiol. 2003; 24:553–554. [PubMed: 12695178]
123. Mitchell P, Birchall D, Mendelow AD. Blood pressure, fatigue, and the pathogenesis of aneurysmal subarachnoid hemorrhage. Surg Neurol. 2006; 66:574–580. [PubMed: 17145314]
124. Moritake K, Handa H, Okumura A, Hayashi K, Nimi H. Stiffness of cerebral arteries--its role in the pathogenesis of cerebral aneurysms. Neurol Med Chir (Tokyo). 1974; 14:47–53. [PubMed: 4143466]
125. Nader-Sepahi A, Casimiro M, Sen J, Kitchen ND. Is aspect ratio a reliable predictor of intracranial aneurysm rupture? Neurosurgery. 2004; 54:1343–1347. [PubMed: 15157290]
126. Nahed BV, Bydon M, Ozturk AK, Bilguvar K, Bayrakli F, Gunel M. Genetics of intracranial aneurysms. Neurosurgery. 2007; 60:213–225. [PubMed: 17290171]
127. Nakatani H, Hashimoto N, Kang Y, Yamazoe N, Kikuchi H, Yamaguchi S, Niimi H. Cerebral blood flow patterns at major vessel bifurcations and aneurysms in rats. J Neurosurg. 1991; 74:258–262. [PubMed: 1988596]
128. Nüssel F, Wegmüller H, Huber P. Morphological and haemodynamic aspects of cerebral aneurysms. Acta Neurochir (Wien). 1993; 120:1–6. [PubMed: 8434510]
129. Ohshima T, Miyachi S, Hattori K, Takahashi I, Ishii K, Izumi T, Yoshida J. Risk of aneurysmal rupture: the importance of neck orifice positioning-assessment using computational flow simulation. Neurosurgery. 2008; 62:767–773. [PubMed: 18496182]
130. Ozdamar N, Celebi G. Pressure distribution on the wall of experimental aneurysms. Acta Neurochir (Wien). 1978; 45:27–34. [PubMed: 742437]
131. Paal G, Ugron A, Szikora I, Bojtar I. Flow in simplified and real models of intracranial aneurysms. International Journal of Heat and Fluid Flow. 2007; 28:653–664.
132. Passerini, Tiziano; Sangalli, Laura M.; Vantini, Simone; Piccinelli, Marina; Bacigaluppi, Susanna; Antiga, Luca; Boccardi, Edoardo; Secchi, Piercesare; Veneziani, Alessandro. An Integrated Statistical Investigation of Internal Carotid Arteries of Patients Affected by Cerebral Aneurysms. Cardiovascular Engineering and Technology. 2012; 3:26–40.
133. Penn DL, Komotar RJ, Sander Connolly E. Hemodynamic mechanisms underlying cerebral aneurysm pathogenesis. J Clin Neurosci. 2011; 18:1435–1438. [PubMed: 21917457]
134. Perktold K, Peter R, Resch M. Pulsatile non-Newtonian blood flow simulation through a bifurcation with an aneurysm. Biorheology. 1989; 26:1011–1030. [PubMed: 2624892]
135. Perktold K, Gruber K, Kenner T, Florian H. Calculation of pulsatile flow and particle paths in an aneurysm-model. Basic Res Cardiol. 1984; 79:253–261. [PubMed: 6477378]
136. Perktold K, Kenner T, Hilbert D, Spork B, Florian H. Numerical blood flow analysis: arterial bifurcation with a saccular aneurysm. Basic Res Cardiol. 1988; 83:24–31. [PubMed: 3377740]
137. Peters DG, Kassam AB, Feingold E, Heidrich-O'Hare E, Yonas H, Ferrell RE, Brufsky A. Molecular anatomy of an intracranial aneurysm: coordinated expression of genes involved in wound healing and tissue remodeling. Stroke. 2001; 32:1036–1042. [PubMed: 11283408]
138. Piccinelli M, Steinman DA, Hoi Y, Tong F, Veneziani A, Antiga L. Automatic Neck Plane Detection and 3D Geometric Characterization of Aneurysmal Sacs. Ann Biomed Eng. 2012 Online before print.
139. Piccinelli M, Veneziani A, Steinman DA, Remuzzi A, Antiga L. A framework for geometric analysis of vascular structures: application to cerebral aneurysms. IEEE Trans Med Imaging. 2009; 28:1141–1155. [PubMed: 19447701]
140. Qiao Y, Steinman DA, Qin Q, Etesami M, Schär M, Astor BC, Wasserman BA. Intracranial arterial wall imaging using three-dimensional high isotropic resolution black blood MRI at 3.0 Tesla. J Magn Reson Imaging. 2011; 34:22–30. [PubMed: 21698704]
141. Raghavan ML, Ma B, Harbaugh RE. Quantified aneurysm shape and rupture risk. J Neurosurg. 2005; 102:355–362. [PubMed: 15739566]

142. Rahman M, Smietana J, Hauck E, Hoh B, Hopkins N, Siddiqui A, Levy EI, Meng H, Mocco J. Size ratio correlates with intracranial aneurysm rupture status: a prospective study. Stroke. 2010; 41:916–920. [PubMed: 20378866]

143. Ramalho S, Moura A, Gambaruto AM, Sequeira A. Sensitivity to outflow boundary conditions and level of geometry description for a cerebral aneurysm. International Journal for Numerical Methods in Biomedical Engineering. 2012; 28:697–713.

144. Rayz VL, Boussel L, Ge L, Leach JR, Martin AJ, Lawton MT, McCulloch C, Saloner D. Flow residence time and regions of intraluminal thrombus deposition in intracranial aneurysms. Ann Biomed Eng. 2010; 38:3058–3069. [PubMed: 20499185]

145. Richardson JC, Hyland HH. Intracranial aneurysms: A clinical and pathological study of subarachnoid and intracerebral haemorrhage caused berry aneurysms. Medicine. 1941; 20:1–83.

146. Rinkel GJ, Djibuti M, Algra A, van Gijn J. Prevalence and risk of rupture of intracranial aneurysms: a systematic review. Stroke. 1998; 29:251–256. [PubMed: 9445359]

147. Roach MR. A model study of why some intracranial aneurysms thrombose but others rupture. Stroke. 1978; 9:583–587. [PubMed: 741491]

148. Roach MR, Scott S, Ferguson GG. The hemodynamic importance of the geometry of bifurcations in the circle of Willis (glass model studies). Stroke. 1972; 3:255–267. [PubMed: 5034974]

149. Robertson AM, Watton PN. Computational fluid dynamics in aneurysm research: critical reflections, future directions. AJNR Am J Neuroradiol. 2012; 33:992–995. [PubMed: 22653325]

150. Ruigrok YM, Rinkel GJ, van't Slot R, Wolfs M, Tang S, Wijmenga C. Evidence in favor of the contribution of genes involved in the maintenance of the extracellular matrix of the arterial wall to the development of intracranial aneurysms. Hum Mol Genet. 2006; 15:3361–3368. [PubMed: 17038484]

151. Ruigrok YM, Rinkel GJ, Wijmenga C. Genetics of intracranial aneurysms. Lancet Neurol. 2005; 4:179–189. [PubMed: 15721828]

152. Ruiz-Sandoval JL, Cantú C, Chiquete E, León-Jiménez C, Arauz A, Murillo-Bonilla LM, Villarreal-Careaga J, Barinagarrementería F. Aneurysmal subarachnoid hemorrhage in a Mexican multicenter registry of cerebrovascular disease: the RENAMEVASC study. J Stroke Cerebrovasc Dis. 2009; 48–55:48–55.

153. Sadatomo T, Yuki K, Migita K, Taniguchi E, Kodama Y, Kurisu K. Morphological differences between ruptured and unruptured cases in middle cerebral artery aneurysms. Neurosurgery. 2008; 62:602–609. [PubMed: 18301349]

154. San Millán Ruíz D, Yilmaz H, Dehdashti AR, Alimenti A, de Tribolet N, Rüfenacht DA. The perianeurysmal environment: influence on saccular aneurysm shape and rupture. AJNR Am J Neuroradiol. 2006; 27:504–512. [PubMed: 16551985]

155. Sato K, Imai Y, Ishikawa T, Matsuki N, Yamaguchi T. The importance of parent artery geometry in intra-aneurysmal hemodynamics. Med Eng Phys. 2008; 30:774–782. [PubMed: 18767212]

156. Schievink WI. Intracranial aneurysms. N Engl J Med. 1997; 336:28–40. [PubMed: 8970938]

157. Sekhar LN, Sclabassi RJ, Sun M, Blue HB, Wasserman JF. Intra-aneurysmal pressure measurements in experimental saccular aneurysms in dogs. Stroke. 1988; 19:352–356. [PubMed: 3354022]

158. Sforza DM, Putman CM, Cebral JR. Computational fluid dynamics in brain aneurysms. International Journal for Numerical Methods in Biomedical Engineering. 2012; 28:801–808.

159. Sforza DM, Putman CM, Cebral JR. Hemodynamics of Cerebral Aneurysms. Annu Rev Fluid Mech. 2009; 41:91–107. [PubMed: 19784385]

160. Shimogonya Y, Ishikawa T, Imai Y, Matsuki N, Yamaguchi T. Can temporal fluctuation in spatial wall shear stress gradient initiate a cerebral aneurysm? A proposed novel hemodynamic index, the gradient oscillatory number (GON). J Biomech. 2009; 42:550–554. [PubMed: 19195658]

161. Shojima M, Oshima M, Takagi K, Torii R, Hayakawa M, Katada K, Morita A, Kirino T. Magnitude and role of wall shear stress on cerebral aneurysm: computational fluid dynamic study of 20 middle cerebral artery aneurysms. Stroke. 2004; 35:2500–2505. [PubMed: 15514200]

162. Shojima M, Oshima M, Takagi K, Torii R, Nagata K, Shirouzu I, Morita A, Kirino T. Role of the bloodstream impacting force and the local pressure elevation in the rupture of cerebral aneurysms. Stroke. 2005; 36:1933–1938. [PubMed: 16081858]
163. Stehbens WE. Aneurysms and anatomical variation of cerebral arteries. Arch Pathol. 1963; 75
164. Stehbens WE. Etiology of intracranial berry aneurysms. J Neurosurg. 1989; 70:823–831. [PubMed: 2654334]
165. Stehbens WE, Martin BJ, Delahunt B. Light and scanning electron microscopic changes observed in experimental arterial forks of rabbits. Int J Exp Pathol. 1991; 72:183–193. [PubMed: 2015201]
166. Steiger HJ. Pathophysiology of development and rupture of cerebral aneurysms. Acta Neurochir Suppl (Wien). 1990; 48:1–57. [PubMed: 2389684]
167. Steiger HJ, Aaslid R, Keller S, Reulen HJ. Strength, elasticity and viscoelastic properties of cerebral aneurysms. Heart Vessels. 1989; 5:41–46. [PubMed: 2584177]
168. Steiger HJ, Poll A, Liepsch D, Reulen HJ. Basic flow structure in saccular aneurysms: a flow visualization study. Heart Vessels. 1987; 3:55–65. [PubMed: 3500943]
169. Steiger HJ, Poll A, Liepsch D, Reulen HJ. Haemodynamic stress in lateral saccular aneurysms. An experimental study. Acta Neurochir (Wien). 1987; 86:98–105. [PubMed: 3630787]
170. Steinman, DA. Assumptions in modelling of large artery hemodynamics. In: Ambrosi, D.; Quarteroni, A.; Rozza, G., editors. Modelling of Physiological Flows. Springer; 2011. p. 1-18.
171. Steinman DA, Milner JS, Norley CJ, Lownie SP, Holdsworth DW. Image-based computational simulation of flow dynamics in a giant intracranial aneurysm. AJNR Am J Neuroradiol. 2003; 24:559–566. [PubMed: 12695182]
172. Stewart, RW. Turbulence. In: NCf.F.M. Films. , editor. Illustrated experiments in fluid mechanics: the NCFMF book of film notes. Cambridge, MA: MIT Press; 1972.
173. Stewart SFC, Paterson EG, Burgreen GW, Hariharan P, Giarra M, Reddy V, Day SW, Manning KB, Deutsch S, Berman MR, Myers MR, Malinauskas RA. Assessment of CFD Performance in Simulations of an Idealized Medical Device: Results of FDA's First Computational Interlaboratory Study. Cardiovascular Engineering and Technology. 2012; 3:139–160.
174. Strother CM. In vitro study of haemodynamics in a giant saccular aneurysm model: influence of flow dynamics in the parent vessel and effects of coil embolisation. Neuroradiology. 1995; 37:159–161. [PubMed: 7761006]
175. Strother CM, Graves VB, Rappe A. Aneurysm hemodynamics: an experimental study. AJNR Am J Neuroradiol. 1992; 13:1089–1095. [PubMed: 1636518]
176. Suzuki J, Ohara H. Clinicopathological study of cerebral aneurysms Origin, rupture, repair, and growth. J Neurosurg. 1978; 48:505–514. [PubMed: 632875]
177. Szikora I, Paal G, Ugron A, Nasztanovics F, Marosfoi M, Berentei Z, Kulcsar Z, Lee W, Bojtar I, Nyary I. Impact of aneurysmal geometry on intraaneurysmal flow: a computerized flow simulation study. Neuroradiology. 2008; 50:411–421. [PubMed: 18180916]
178. Takao H, Murayama Y, Otsuka S, Qian Y, Mohamed A, Masuda S, Yamamoto M, Abe T. Hemodynamic differences between unruptured and ruptured intracranial aneurysms during observation. Stroke. 2012; 43:1436–1439. [PubMed: 22363053]
179. Tanoue T, Tateshima S, Villablanca JP, Viñuela F, Tanishita K. Wall shear stress distribution inside growing cerebral aneurysm. AJNR Am J Neuroradiol. 2011; 32:1732–1737. [PubMed: 21984256]
180. Tateshima S, Viñuela F, Villablanca JP, Murayama Y, Morino T, Nomura K, Tanishita K. Three-dimensional blood flow analysis in a wide-necked internal carotid artery-ophthalmic artery aneurysm. J Neurosurg. 2003; 99:526–533. [PubMed: 12959441]
181. Tateshima S, Chien A, Sayre J, Cebral J, Viñuela F. The effect of aneurysm geometry on the intra-aneurysmal flow condition. Neuroradiology. 2010; 52:1135–1141. [PubMed: 20373097]
182. Tateshima S, Murayama Y, Villablanca JP, Morino T, Nomura K, Tanishita K, Viñuela F. In vitro measurement of fluid-induced wall shear stress in unruptured cerebral aneurysms harboring blebs. Stroke. 2003; 34:187–192. [PubMed: 12511772]
183. Tateshima S, Tanishita K, Omura H, Villablanca JP, Vinuela F. Intra-aneurysmal hemodynamics during the growth of an unruptured aneurysm: in vitro study using longitudinal CT angiogram database. AJNR Am J Neuroradiol. 2007; 28:622–627. [PubMed: 17416810]

184. Tezduyar TE, Takizawa K, Brummer T, Chen PR. Space-time fluid-structure interaction modeling of patient-specific cerebral aneurysms. International Journal for Numerical Methods in Biomedical Engineering. 2011; 27:1665–1710.

185. Torii R, Oshima M, Kobayashi T, Kobayashi T, Takagi K, Tezduyar TE. Influence of wall thickness on fluid-structure interaction computations of cerebral aneurysms. International Journal for Numerical Methods in Biomedical Engineering. 2010; 26:336–347.

186. Torii R, Oshima M, Kobayashi T, Takagi K, Tezduyar TE. Fluid-structure interaction modeling of blood flow and cerebral aneurysm: Significance of artery and aneurysm shapes. Computer Methods in Applied Mechanics and Engineering. 2009; 198:3613–3621.

187. Toth BK, Nasztanovics F, Bojtar I. Laboratory tests for strength parameters of brain aneurysms. Acta Bioeng Biomech. 2007; 9:3–7. [PubMed: 18421937]

188. Tremmel M, Dhar S, Levy EI, Mocco J, Meng H. Influence of intracranial aneurysm-to-parent vessel size ratio on hemodynamics and implication for rupture: results from a virtual experimental study. Neurosurgery. 2009; 64:622–630. [PubMed: 19349824]

189. Tulamo R, Frösen J, Hernesniemi J, Niemelä M. Inflammatory changes in the aneurysm wall: a review. J Neurointerv Surg. 2010; 2:120–130. [PubMed: 21990591]

190. Turner CL, Tebbs S, Smielewski P, Kirkpatrick PJ. The influence of hemodynamic stress factors on intracranial aneurysm formation. J Neurosurg. 2001; 95:764–770. [PubMed: 11702865]

191. Ujiie H, Liepsch DW, Goetz M, Yamaguchi R, Yonetani H, Takakura K. Hemodynamic study of the anterior communicating artery. Stroke. 1996; 27:2086–2093. [PubMed: 8898821]

192. Ujiie H, Tachibana H, Hiramatsu O, Hazel AL, Matsumoto T, Ogasawara Y, Nakajima H, Hori T, Takakura K, Kajiya F. Effects of size and shape (aspect ratio) on the hemodynamics of saccular aneurysms: a possible index for surgical treatment of intracranial aneurysms. Neurosurgery. 1999; 45:119–129. [PubMed: 10414574]

193. Ujiie H, Tamano Y, Sasaki K, Hori T. Is the aspect ratio a reliable index for predicting the rupture of a saccular aneurysm? Neurosurgery. 2001; 48:495–502. [PubMed: 11270538]

194. Valen-Sendstad K, Mardal KA, Mortensen M, Reif BAP, Langtangen HP. Direct numerical simulation of transitional flow in a patient-specific intracranial aneurysm. Journal of Biomechanics. 2011; 44:2826–2832. [PubMed: 21924724]

195. Valencia A, Ledermann D, Rivera R, Bravo E, Galvez M. Blood flow dynamics and fluid-structure interaction in patient-specific bifurcating cerebral aneurysms. International Journal for Numerical Methods in Fluids. 2008; 58:1081–1100.

196. Valencia AA, Guzma'n AM, Finol EA, Amon CH. Blood flow dynamics in saccular aneurysm models of the basilar artery. J Biomech Eng. 2006; 128:516–526. [PubMed: 16813443]

197. van Dyke, M. An Album of Fluid Motion. Stanford, CA: Parabolic Press; 1982.

198. van Ooij P, Guédon A, Poelma C, Schneiders J, Rutten MC, Marquering HA, Majoie CB, VanBavel E, Nederveen AJ. Complex flow patterns in a real-size intracranial aneurysm phantom: phase contrast MRI compared with particle image velocimetry and computational fluid dynamics. NMR Biomed. 2012; 25:14–26. [PubMed: 21480417]

199. van Ooij P, Zwanenburg JJ, Visser F, Majoie CB, Vanbavel E, Hendrikse J, Nederveen AJ. Quantification and visualization of flow in the Circle of Willis: Time-resolved three-dimensional phase contrast MRI at 7 T compared with 3 T. Magn Reson Med. 2012 Online before print.

200. Venkatesh B, Shen Q, Lipman J. Continuous measurement of cerebral blood flow velocity using transcranial Doppler reveals significant moment-to-moment variability of data in healthy volunteers and in patients with subarachnoid hemorrhage. Critical Care Medicine. 2002; 30:563–569. [PubMed: 11990915]

201. Venugopal P, Valentino D, Schmitt H, Villablanca JP, Viñuela F, Duckwiler G. Sensitivity of patient-specific numerical simulation of cerebal aneurysm hemodynamics to inflow boundary conditions. J Neurosurg. 2007; 106:1051–1060. [PubMed: 17564178]

202. Vignon-Clementel IE, Figuero CA, Jansen KE, Taylor CA. Outflow boundary conditions for 3D simulations of non-periodic blood flow and pressure fields in deformable arteries. Comput Methods Biomech Biomed Engin. 2010; 13:625–640. [PubMed: 20140798]

203. Watton PN, Selimovic A, Raberger NB, Huang P, Holzapfel GA, Ventikos Y. Modelling evolution and the evolving mechanical environment of saccular cerebral aneurysms. Biomech Model Mechanobiol. 2011; 10:109–132. [PubMed: 20496095]
204. Weir B. Unruptured intracranial aneurysms: a review. J Neurosurg. 2002; 96:3–42. [PubMed: 11794601]
205. Weller RO. Subarachnoid haemorrhage and myths about saccular aneurysms. J Clin Pathol. 1995; 48:1078–1081. [PubMed: 8567990]
206. Wiebers DO. Unruptured intracranial aneurysms: natural history clinical management. Update on the international study of unruptured intracranial aneurysms. Neuroimaging Clin N Am. 2006; 16:383–390. [PubMed: 16935706]
207. Wiebers DO, Whisnant JP, Sundt TM Jr, O'Fallon WM. The significance of unruptured intracranial saccular aneurysms. J Neurosurg. 1987; 66:23–29. [PubMed: 3783255]
208. Wilson G, Riggs HE, Rupp C. The pathologic anatomy of ruptured cerebral aneurysms. J Neurosurg. 1954; 11:128–134. [PubMed: 13152563]
209. Wong GK, Poon WS. Current status of computational fluid dynamics for cerebral aneurysms: the clinician's perspective. J Clin Neurosci. 2011; 18:1285–1288. [PubMed: 21795051]
210. Xiang J, Tremmel M, Kolega J, Levy EI, Natarajan SK, Meng H. Newtonian viscosity model could overestimate wall shear stress in intracranial aneurysm domes and underestimate rupture risk. J Neurointerv Surg. 2011; 4:351–357. [PubMed: 21990529]
211. Yamaguchi R, Ujiie H, Haida S, Nakazawa N, Hori T. Velocity profile and wall shear stress of saccular aneurysms at the anterior communicating artery. Heart Vessels. 2008; 23:60–66. [PubMed: 18273548]
212. Yasuda R, Strother CM, Taki W, Shinki K, Royalty K, Pulfer K, Karmonik C. Aneurysm volume-to-ostium area ratio: a parameter useful for discriminating the rupture status of intracranial aneurysms. Neurosurgery. 2011; 68:310–317. [PubMed: 21135739]
213. Zhang B, Fugleholm K, Day LB, Ye S, Weller RO, Day IN. Molecular pathogenesis of subarachnoid haemorrhage. Int J Biochem Cell Biol. 2003; 35:1341–1360. [PubMed: 12798348]
214. Zhao X, Raghavan ML, J Lu. Characterizing heterogeneous properties of cerebral aneurysms with unknown stress-free geometry: a precursor to in vivo identification. J Biomech Eng. 2011; 133:051008. [PubMed: 21599099]
215. Zhuang YJ, Singh TM, Zarins CK, Masuda H. Sequential increases and decreases in blood flow stimulates progressive intimal thickening. Eur J Vasc Endovasc Surg. 1998; 16:301–310. [PubMed: 9818007]

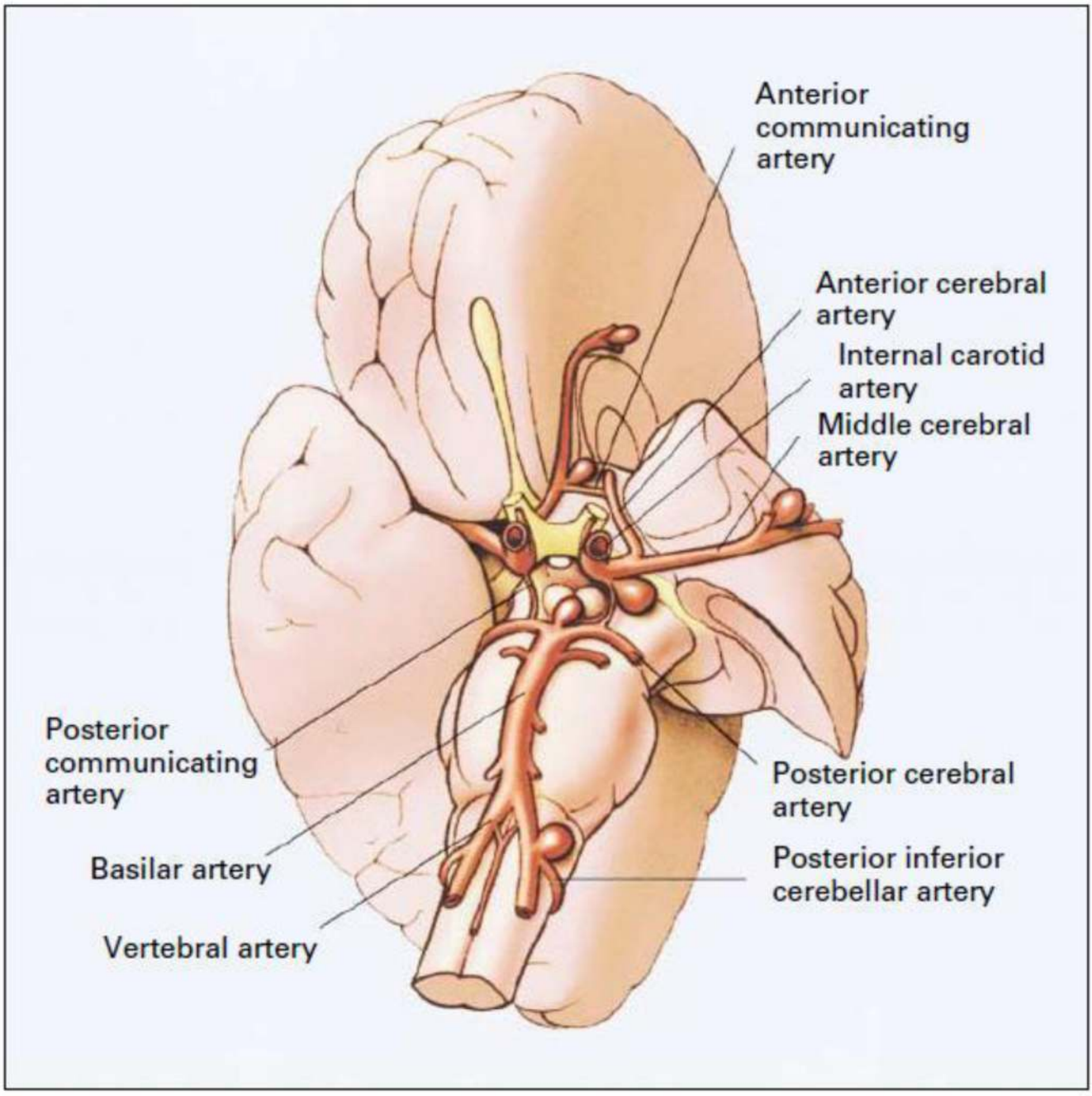

Figure 1.
Circle of Willis showing common locations of cerebral aneurysms. From Schievink 1997[156](N. Engl. J. Med., Schievink WI, Intracranial aneurysms, 336, pp.29, Copyright ©1997 Massachusetts Medical Society. Reprinted with permission from Massachusetts Medical Society)

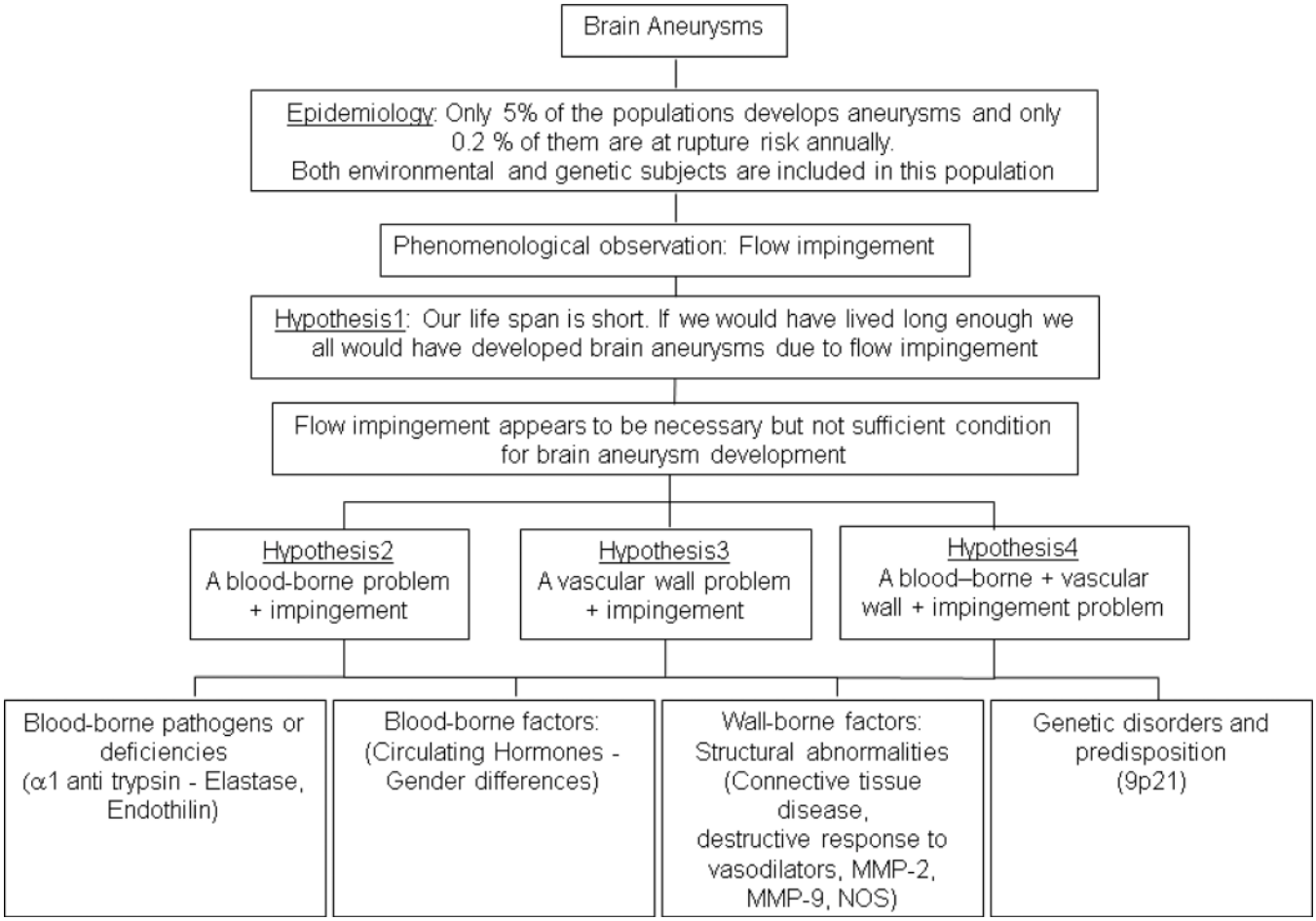

Figure 2.
A basic flowchart showing mechanistic possibilities of aneurysm pathophysiology

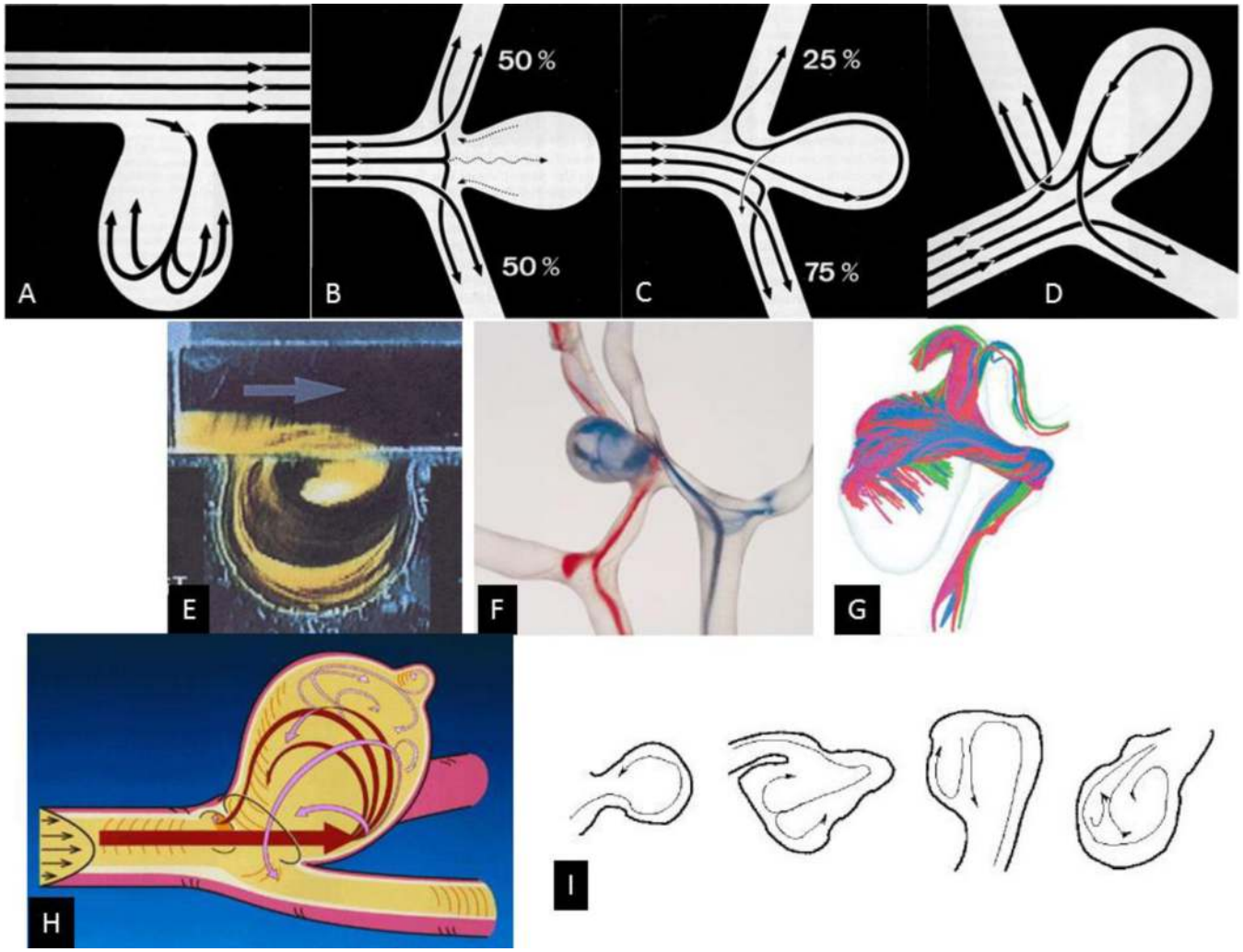

Figure 3.

Schematics of flow patterns in A) sidewall, B) bifurcation with symmetrical outflow, C) bifurcation with asymmetrical outflow, and D) asymmetric bifurcation. E) Laser induced fluorescence study in a sidewall channel at mid systolic acceleration; F) Dye visualization in an elastomer model of an anterior communicating artery aneurysm; asymmetrical internal carotid flow; G) Computational fluid dynamics in a giant internal carotid-posterior communicating artery aneurysm at early diastole; H) schematic of flow patterns in a high aspect ratio bifurcation aneurysm with a bleb; I) schematic at one instant in the cardiac cycle of different flow patterns obtained from computational fluid dynamics simulations in anatomically realistic aneurysms. Panels A–D from Steiger 1987[168] (With kind permission from Springer Science+Business Media: Heart Vessels, Basic flow structure in saccular aneurysms, 3, 1987, pp.57–61, Steiger HJ et al., Figures 3,7a,7b,8); panel E from Lieber 1997[107] (With kind permission from Springer Science+Business Media: Ann. Biomed. Eng., Alteration of hemodynamics in aneurysm models by stenting, 25, 1997, pp.463, Lieber BB et al., Figure 5A); panel F from Kerber 1999[92] (CW Kerber et al., Flow dynamics in a lethal anterior communicating artery aneurysm, AJNR Am J Neuroradiol, 20, 10, pp.2000–3, 1999 © by American Society of Neuroradiology); panel G from Steinman 2003[171] (DA Steinman et al., Image-based computational simulation of flow dynamics in a giant intracranial aneurysm, AJNR Am J Neuroradiol, 24, 4, pp.559–66, 2003 © by American Society of Neuroradiology); panel H from Ujiie 1999[192] (Ujiie H et al., Effects of size and shape

(aspect ratio) on the hemodynamics of saccular aneurysms, Neurosurgery, 45, 1, pp.119-29, 1999); panel I from Cebral 2005[23] (JR Cebral et al., Characterization of cerebral aneurysms for assessing risk of rupture by using patient-specific computational hemodynamics models, AJNR Am J Neuroradiol, 26, 10, pp.2550–9, 2005 © by American Society of Neuroradiology)

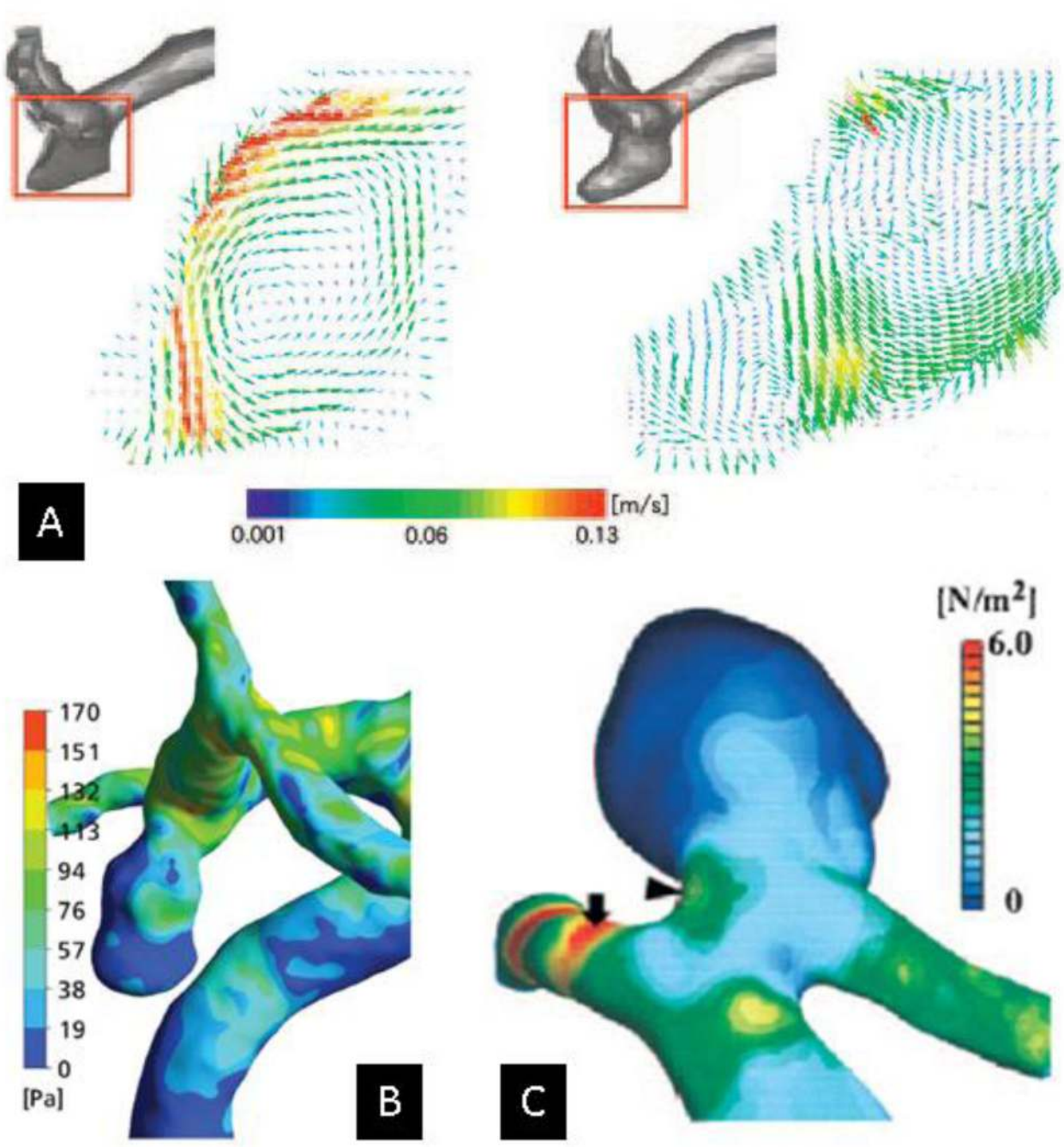

Figure 4.

A) Velocity vectors obtained with laser Doppler velocimetry in acrylic casts of a middle cerebral artery aneurysm before and after it grew over a period of 1 year. Examples of wall shear stress magnitudes calculated with computational fluid dynamics in B) a posterior communicating artery and C) a middle cerebral artery aneurysm. Panel A from Tateshima 2007[183] (S Tateshima et al., Intra-aneurysmal hemodynamics during the growth of an unruptured aneurysm, AJNR Am J Neuroradiol, 28, 4, pp.622–7, 2007 © by American Society of Neuroradiology); Panel B from Kulcsár 2011[101] (Z Kulcsár, et al., I Szikora, Hemodynamics of cerebral aneurysm initiation, AJNR Am J Neuroradiol, 32, 3, pp.587–94, 2011 © by American Society of Neuroradiology); Panel C from Shojima 2004[161] (Shojima

M et al., Magnitude and role of wall shear stress on cerebral aneurysm, Stroke, 35, 11, pp. 2500–5, 2004)

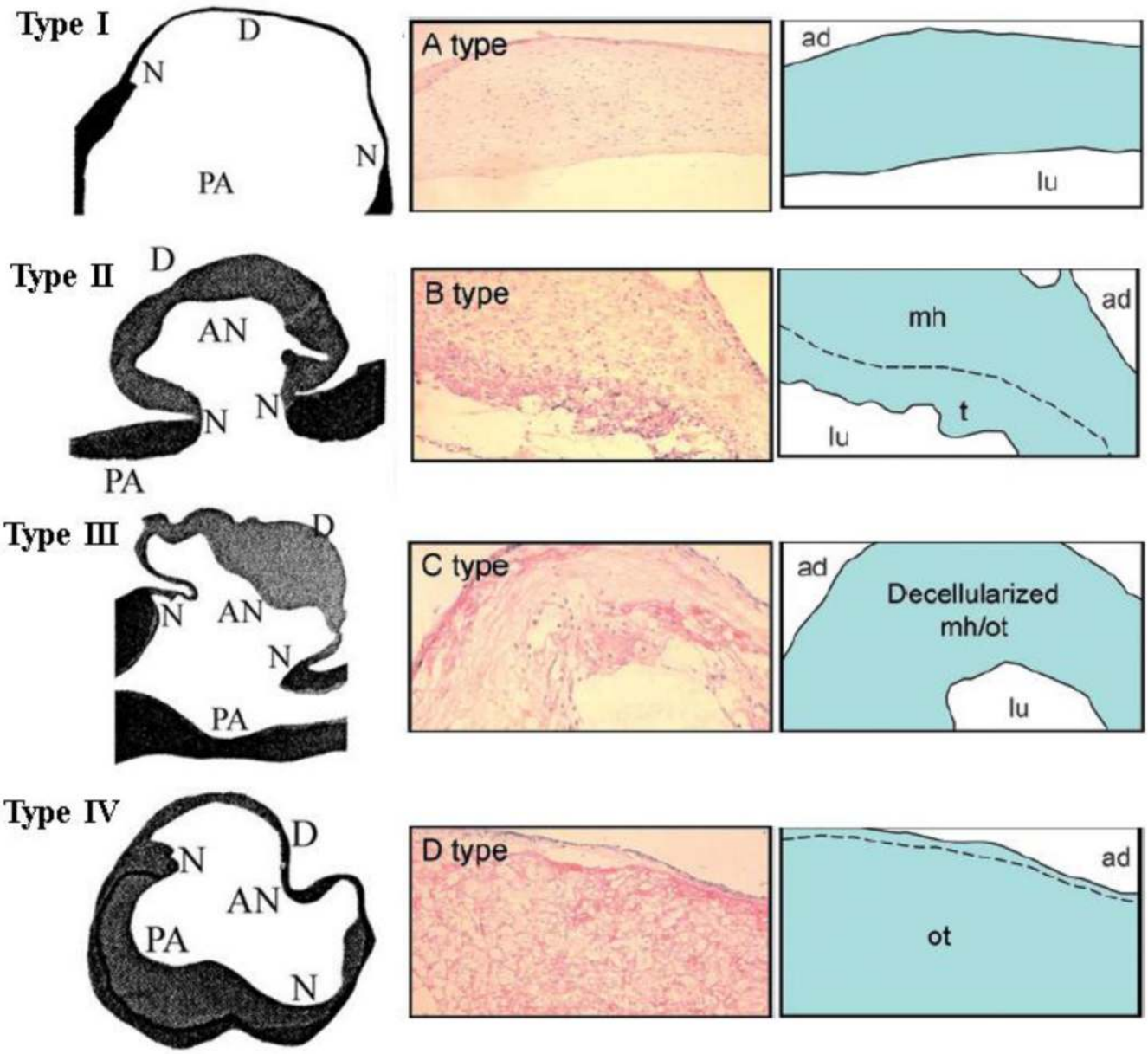

Figure 5.

Four different types of aneurysm wall generally characterizing changes during progression to rupture. AN: aneurysm; PA: parent artery; N: neck; D: dome; ad: adventitial side; lu: luminal side; mh: myointimal hyperplasia; t: fresh thrombus; ot: organizing thrombus Left column with types I–IV from Suzuki 1978[176] (Suzuki J and Ohara H, Clinicopathological study of cerebral aneurysms, J. Neurosurg., 48, pp.505–14, 1978); right columns with types A–D from Tulamo 2010[189] (Adapted by permission from BMJ Publishing Group Limited. [J. Neurointerv. Surg., Tulamo R, Frösen J, Hernesniemi J, Niemelä M, 2, pp.120–30, 2010])

Table 1

The location of aneurysms on the circle of Willis

Article	Number of aneurysms	ICA (%)	MCA (%)	ACA (%)	PComA (%)	AComA (%)	Basilar (%)
Crawford 1959[30]	163	30 (18)	54 (34)	20 (12)	–	46 (28)	7 (4)
Kayembe 1984[91]	67	12 (18)	15 (22)	2 (3)	–	27 (40)	4 (6)
Rinkel 1998[a], [146]	563	223 (42)	159 (30)	126 (24)	–	–	55 (10)[b]
Forget 2001[46]	245	27 (11)	29 (12)	–	48 (20)	71 (29)	36 (15)
Joo 2009[78]	889	131 (15)	258 (29)	–	152 (17)	284 (32)	–
Jeong 2009[76]	239	20 (8)	61 (25)	14 (6)	52 (22)	66 (28)	13 (5)
De Rooij 2009[34]	150	10 (7)	84 (56)	–	20 (13)	22 (15)	14 (9)
Carter 2006[17]	1673	216 (13)	398 (24)	–	315 (19)	426 (26)	193 (12)
Ruiz- Sandoval 2009[152]	231	42 (18)	46 (20)	–	64 (28)	61 (26)	7 (3)
Hademenos 1998[59]	74	18 (24)	3 (4)	–	11 (15)	4 (5)	24 (32)
Richardson 1941[145]	53	13 (25)	16 (30)	–	–	13 (25)	6 (11)
Nader- Sepahi 2004[125]	182	23 (13)	53 (29)	–	47 (26)	28 (15)	–
Juvela 2000[81]	181	79 (44)	82 (45)	7 (4)	–	8 (4)	5 (3)
Weir 2002[a], [204]	3776	1437 (38)	797 (21)	–	–	1118 (30)	234 (6)[b]
McDonald 1939[120]	1023	165 (16)	294 (29)	121 (9)	66 (6)	158 (15)	143 (14)
Beck 2006[9]	155	19 (12)	39 (25)	49 (32)[c]	20 (13)	–	28 (18)
Baharoglu 2012[4]	271	52 (19)	40 (15)	5 (2)	49 (18)	58 (21)	12 (4)
Mackey 2012[116]	2930	1067 (36)	749 (26)	398 (14)[c]	374 (13)	–	342 (12)
Mean±Std Dev. %		**21±11%**	**26±12%**	**12±10%**	**17±6%**	**23±10%**	**10±7%**

[a] Literature review

[b] Posterior circulation

[c] Includes AcomA

Table 2

Differences in size of ruptured and unruptured aneurysms

Article	Ruptured (mm)	Unruptured (mm)	Effect size (mm)	Effect Size (% of ruptured size)
Sadatomo 2008[153]	7.2	5.6	1.6	22%
Baharoglu 2012[4]	7.8	6.4	1.4	18%
Weir 2002 (in Lall 2009[102])	8	7	1	13%
Weir 2003 (in Lall 2009[102])	10.8	7.8	3	28%
Hoh 2007 (in Lall 2009[102])	6.2	4.3	1.9	31%
Juvela 2008 (in Lall 2009[102])	5.6	4.9	0.7	13%
Baumann 2008 (in Lall 2009[102])	7	4	3	43%
Beck 2006[9]	6.7	5.7	1	15%
Yasuda 2011[212]	6.7	4.9	1.8	27%
Hademenos 1998[59]	11.9	13.5	−1.6	−13%
Juvela 2000	5.6	4.9	0.7	13%
de la Monte 1985 (in Weir 2002[204])	11.4	7.6	3.8	33%
Nader-Sepahi 2004[125]	7.7	5.1	2.6	34%
Carter 2006[17]	8.2	8.4	−0.2	−2%
Rahman 2010[142]	7.9	6.2	1.7	22%
San Millán Ruíz 2006[154]	7.6	6.1	1.5	20%
Joo 2009[78]	6.3	5.5	0.8	13%
Mean(std.error)			1.5(0.3)	19(3)%